EuroIntervention
2026;22:e74-e89
published online e-edition January 2026
DOI: 10.4244/EIJ-D-25-00266

State-of-the-Art
by EuroIntervention

Lesion stratification with intracoronary imaging

Michael McGarvey[1,2], MA, MBBS; Kalpa De Silva[2,3], MBBS, PhD; Thomas R. Keeble[4,5], MBBS, MD; Thomas W. Johnson[6], BSc, MBBS, MD; Peter O'Kane[7], MBBS, MD; Ziad A. Ali[8,9], MD, DPhil; Shengxian Tu[10,11], PhD; Sundeep Kalra[12], PhD; Divaka Perera[2,3], MD; Philip MacCarthy[1,2], BSc, PhD; Jonathan M. Hill[13], MD; Jonathan Byrne[1,2], BSc, PhD; Rafal Dworakowski[1,2,14], PhD; Nilesh Pareek[1,2]*, MA, PhD

Corresponding author: School of Cardiovascular and Metabolic Medicine and Sciences, BHF Centre of Excellence, James Black Centre, 125 Coldharbour Lane, London, SE5 9NU, United Kingdom. E-mail: nileshpareek@nhs.net

This paper also includes supplementary data published online at: https://eurointervention.pcronline.com/doi/10.4244/EIJ-D-25-00266

ABSTRACT

Intracoronary (IC) imaging-guided percutaneous coronary intervention (PCI) improves clinical outcomes in patients with high clinical and anatomical risk when compared to interventions guided by angiography alone. Recent Class I recommendations for the use of IC imaging guidance when performing PCI in left main stem or complex lesions may result in a significant uptake as the technology is embraced as standard of care. Routine application of IC imaging will provide interventional cardiologists with a wealth of high-fidelity intracoronary data on plaque composition and distribution. When paired with emerging data regarding the importance of plaque anatomical characteristics, developments in artificial intelligence and computational fluid dynamics, lesion stratification with IC imaging may herald the next paradigm shift in this field. In this review, we will explore this important emerging application of IC imaging to inform morphology-guided PCI, identify high-risk lesions for targeted therapies, and consider the prospects of harnessing automated image interpretation with artificial intelligence technologies to achieve an integrated physiological and morphological assessment. Lesion stratification with IC imaging has the potential to shape the future of interventional cardiology practice to guide therapies within and beyond the confines of the cardiac catheterisation laboratory.

Our understanding of atherosclerosis and existing therapeutic approaches have evolved in parallel with technologies to assess and evaluate coronary plaque. Intracoronary (IC) imaging facilitates *in vivo* assessment of the anatomical features of coronary lesions with near-histological precision and has revolutionised our understanding of the mechanisms underpinning both chronic (CCS) and acute coronary syndromes (ACS). Application of IC imaging in clinical practice has primarily concentrated on guidance and optimisation of percutaneous coronary intervention (PCI), with observed reductions in target vessel failure (TVF), target vessel myocardial infarction (TVMI), and all-cause mortality when compared to angiography-guided interventions[1]. Recently, the use of IC imaging to guide PCI for left main stem (LMS) or anatomically complex lesions received a Class I, Level of Evidence A recommendation, and this is likely to lead to a substantial increase in the use of IC imaging[2,3].

Routine assessment of lesion morphological characteristics with IC imaging may offer important additional information, with the potential to transform our understanding of coronary artery disease (CAD) and its therapies across the clinical spectrum. For example, identification of lesions with high-risk characteristics may inform a burgeoning field of targeted therapies to pacify "vulnerable" lesions and prevent future events[4]. Evaluation of culprit lesions in ACS may help to evolve interventional and pharmacological approaches for managing the disease[5]. Finally, through developments in automated IC image interpretation, powered by artificial intelligence (AI) and advances in computational fluid dynamics modelling of coronary flow, IC imaging technologies may now render the dichotomous functional versus morphological approach to lesion stratification redundant.

In this review, we will appraise the evidence and guidelines supporting the current application of IC imaging in clinical care. We will then describe a contemporary approach to

KEYWORDS: intravascular ultrasound; optical coherence tomography; other imaging modalities

© Europa Group 2026. All rights reserved.
SUBMITTED ON 10/03/2025 - REVISION RECEIVED ON 1st 02/06/2025 / 2nd 30/06/2025 - ACCEPTED ON 18/07/2025

the use of IC imaging for assessment and stratification of lesion morphology during PCI planning, emerging concepts of IC imaging-guided therapy in ACS, the characterisation and treatment of the high-risk plaque, and the promise of a complete morphofunctional lesion assessment from IC imaging alone. We are entering an era where IC imaging use for the evaluation and treatment of CAD is likely to become widespread. By embracing its potential, whilst undertaking robust clinical validation, we can shape interventional cardiology practice in the coming decade.

Intracoronary imaging & current international guidelines

Intravascular ultrasound (IVUS) and optical coherence tomography (OCT) are the IC imaging modalities currently used in routine clinical practice. Globally, IC imaging use remains low with substantial geographical variation and barriers to adoption, including concerns about reimbursement, time constraints, and confidence with image interpretation. In Japan, documented rates of IC imaging-guided PCI approach 85%, while in the United States, IC imaging is used to guide just 15-20% of PCI[6].

Since 2015, almost 20,000 patients, across the spectrum of stable and acute syndromes, have been included in international randomised controlled trials (RCTs) comparing IC imaging-guided PCI against angiographic-guided intervention. Taken in concert, these studies clearly demonstrate the superiority of IC imaging over angiography-guided PCI **(Table 1)**[7-14]. International guidelines now state that IC imaging should be used to guide intervention in LMS and anatomically complex lesions, regardless of clinical syndrome (Class I, Level of Evidence A)[2,3].

IC imaging informs interventional device sizing, identification of landing zones, and early correction of prognostically relevant complications, such as stent strut malapposition, stent underexpansion, edge dissection, and inadequate lesion coverage. When compared directly in clinical trials, or indirectly in network meta-analyses, the benefits of using OCT and IVUS to guide and optimise PCI appear equivalent[15]. The choice of IC modality may be guided by the clinical scenario and the relative strengths of each device.

IVUS is preferred in assessment of the LMS due to its ability to assess the ostial segment and its superior depth of penetration. In patients with angiographically intermediate LMS stenoses, assessment with IVUS should be considered to guide revascularisation decision-making (Class IIa, Level of Evidence B)[2]. In an ACS, where there remains ambiguity in identifying the culprit lesion following angiographic assessment, guidelines state that IC imaging (preferably with OCT) should be used to facilitate diagnosis and guide therapeutic decision-making (Class IIb, Level of Evidence C)[16]. In patients with suspected stent failure, however, either OCT or IVUS may be used to detect the causative mechanism and mode of failure (Class IIa, Level of Evidence C)[17].

Lesion characterisation & evolving concepts in PCI planning

IC imaging enables the morphological assessment of plaque characteristics *in vivo*. These technologies have supported an evolution in our understanding of coronary atherosclerosis that may be reliably applied to guide clinical diagnosis, inform lesion stratification, and facilitate procedural planning **(Central illustration)**. Plaque may be categorised as lipid-rich, fibrous, and calcific, with each morphology associated with stereotyped biomechanical properties – *in vivo*, multiple morphologies may coexist within a single lesion, and their relative distribution is an important consideration for interventional strategy planning.

MORPHOLOGICAL CHARACTERISTICS & PCI STRATEGY

Clinically significant calcification is present in approximately 20% of patients undergoing PCI and is associated with adverse clinical outcomes[18]. Vascular calcification impacts the delivery of angioplasty equipment, resists balloon expansion, and results in radial constraint of stents. IC imaging detects calcified plaque with high sensitivity and specificity, and its application in guiding PCI in calcified lesions is associated with increased post-PCI minimum stent area (MSA)[19,20]. Semiquantitative assessment of calcium volume with OCT or IVUS, integrating assessment of calcium arc, depth, length, or morphology, may predict the risk of stent underexpansion **(Supplementary Table 1)**[21-23] and is increasingly integrated into treatment algorithms to guide early escalation to advanced calcium modification techniques[18].

Nodular calcification presents a particular challenge and may be subcategorised into protruding calcified nodules (PCNs) and eruptive calcified nodules (ECNs). PCNs are characterised by a dome-like protrusion into the lumen, with a smooth and intact endothelial layer, whilst ECNs have an irregular surface, endothelial disruption, and overlying fibrin deposition[24]. Despite the application of dedicated modification protocols, ECNs are associated with significantly increased rates of target vessel failure (irrespective of post-PCI MSA), with reported cases of ECNs recurring through previously stented segments[25,26].

Lipid-rich lesions, on the other hand, as detected with OCT and near-infrared spectroscopy (NIRS), are associated with

Abbreviations

ECN	eruptive calcified nodule	**MLA**	minimum lumen area	**RF**	radiofrequency
FFR	fractional flow reserve	**MSA**	minimum stent area	**SCAD**	spontaneous coronary artery dissection
IC	intracoronary	**NIRS**	near-infrared spectroscopy	**TCFA**	thin-cap fibroatheroma
IVUS	intravascular ultrasound	**PCN**	protruding calcified nodule	**VFR**	virtual flow reserve
LCBI	lipid core burden index	**PE**	plaque erosion		
LMS	left main stem	**PR**	plaque rupture		

Table 1. Randomised controlled trials comparing clinical outcomes following PCI guided by intracoronary imaging versus angiography guidance.

Trial	Enrolled, n (Randomisation ratio)	IC imaging modality	Follow-up, months	Lesion complexity	Endpoint	Results	Notes
CTO-IVUS (2015)[7]	402 (1:1)	IVUS vs angio	12	Chronic total occlusion	Composite of cardiac death, TLMI or ischaemia-driven TLR	5 (2.6%) vs 14 (7.1%) (HR 0.35, 95% CI: 0.13-0.97; p=0.035)	Primary outcome was cardiac death; 0 in IVUS group vs 2 in angio-only group Korea only
IVUS-XPL (2015)[8]	1,4 (1:1)	IVUS vs angio	12	Long lesions ≥28 mm	Composite of cardiac death, TLMI or ischaemia-driven TLR	19 (2.9%) vs 39 (5.8%) (HR 0.48, 95% CI: 0.28-0.83; p=0.007)	94.5% follow-up at 12 months Korea only
ULTIMATE (2018)[9]	1,448 (1:1)	IVUS vs angio	12	All-comers 8.9% CTO 12.6% unprotected left main 34.2% any bifurcation Avg. stent length ~48 mm 24.8% moderate to severe Ca^{2+}	Composite of cardiac death, TVMI or clinically indicated TVR	21 (2.9%) vs 39 (5.4%) (HR 0.53, 95% CI: 0.31-0.90; p=0.02)	Minimum operator volume: 200 PCI/yr China only
RENOVATE-COMPLEX-PCI (2023)[10]	1,639 (2:1)	OCT or IVUS vs angio	24	Complex lesions 19.5% CTO 11.7% unprotected left main 21.9% true bifurcation 54.8% long lesion (≥38 mm) 37.9 % multivessel PCI 14.1% severe Ca^{2+}	Composite of cardiac death, TVMI or clinically indicated TVR	76 (7.7%) vs 60 (12.3%) (HR 0.64, 95% CI: 0.45-0.81; p=0.008)	Korea only
OCTOBER (2023)[11]	1,201 (1:1)	OCT vs angio	24	True bifurcations with SB diameter ≥2.5 mm 18.9% LMS 70.5% LAD/D1	Composite of cardiac death, TLMI or ischaemia-driven TLR	59 (10.1%) vs 83 (14.1%) (HR 0.70, 95% CI: 0.50-0.98; p=0.035)	Europe only 15.3% IVUS use in the angiography arm
ILUMIEN IV (2023)[12]	2,487 (1:1)	OCT vs angio	24	Complex lesions and/or T2DM 7.0% CTO 3.4% two-stent bifurcation 67.6% long lesion (≥28 mm) 11.5% severe Ca^{2+} 5.5% STEMI culprit 24.1% non-STEMI culprit	Composite of cardiac death, TVMI or ischaemia-driven TVR	88 (7.4%) vs 99 (8.2%) (HR 0.90, 95% CI: 0.67-1.19; p=0.45)	18 countries in Europe, North America, Asia & Oceania Co-primary endpoint of final MSA was 5.72±2.04 mm^2 vs 5.36±1.87 mm^2 (p<0.0001)
IVUS-ACS (2024)[13]	3,505 (1:1)	IVUS vs angio	12	Acute coronary syndromes 27.6% STEMI 4.3% unprotected left main 15.2% true bifurcation 72.5% long lesion (≥30 mm) 7.6% moderate to severe Ca^{2+}	Composite of cardiac death, TVMI or clinically indicated TVR	70 (4.0%) vs 128 (7.3%) (HR 0.55, 95% CI: 0.41-0.74; p=0.0001)	China (52 centres), Pakistan (2), UK (1), Italy (1) Minimum of 1,000 PCI per site* & 200 PCI per operator Patients underwent a second randomisation to DAPT vs ticagrelor monotherapy
OCCUPI (2024)[14]	1,604 (1:1)	OCT vs angio	12	Complex lesions 7.2% CTO 20.4% acute myocardial infarction 14.3% unprotected left main 23.8% true bifurcation 71.8% long lesion (≥28 mm) 9.3% severe Ca^{2+} 8.1% intracoronary thrombus 10.7% in-stent restenosis	Composite of cardiac death, MI, stent thrombosis, or ischaemia-driven TLR	37 (4.6%) vs 59 (7.4%) (HR 0.62, 95% CI: 0.41-0.93; p=0.023)	Korea only Initial 2x2 factorial analysis with assessment of 3-month DAPT vs 12-month DAPT abandoned due to concern about the lack of equipoise in this cohort

*Except for the UK site. Ca^{2+}: calcification; CI: confidence interval; CTO: chronic total occlusion; D1: first diagonal branch; DAPT: dual antiplatelet therapy; HR: hazard ratio; IC: intracoronary; IVUS: intravascular ultrasound; LAD: left anterior descending artery; LMS: left main stem; MI: myocardial infarction; MSA: minimum stent area; OCT: optical coherence tomography; PCI: percutaneous coronary intervention; SB: side branch; STEMI: ST-segment elevation myocardial infarction; T2DM: Type 2 diabetes mellitus; TLMI: target lesion myocardial infarction; TLR: target lesion revascularisation; TVMI: target vessel myocardial infarction; TVR: target vessel revascularisation

EuroIntervention — Central Illustration

Lesion characteristics stratified according to associated clinical risk & syndrome.

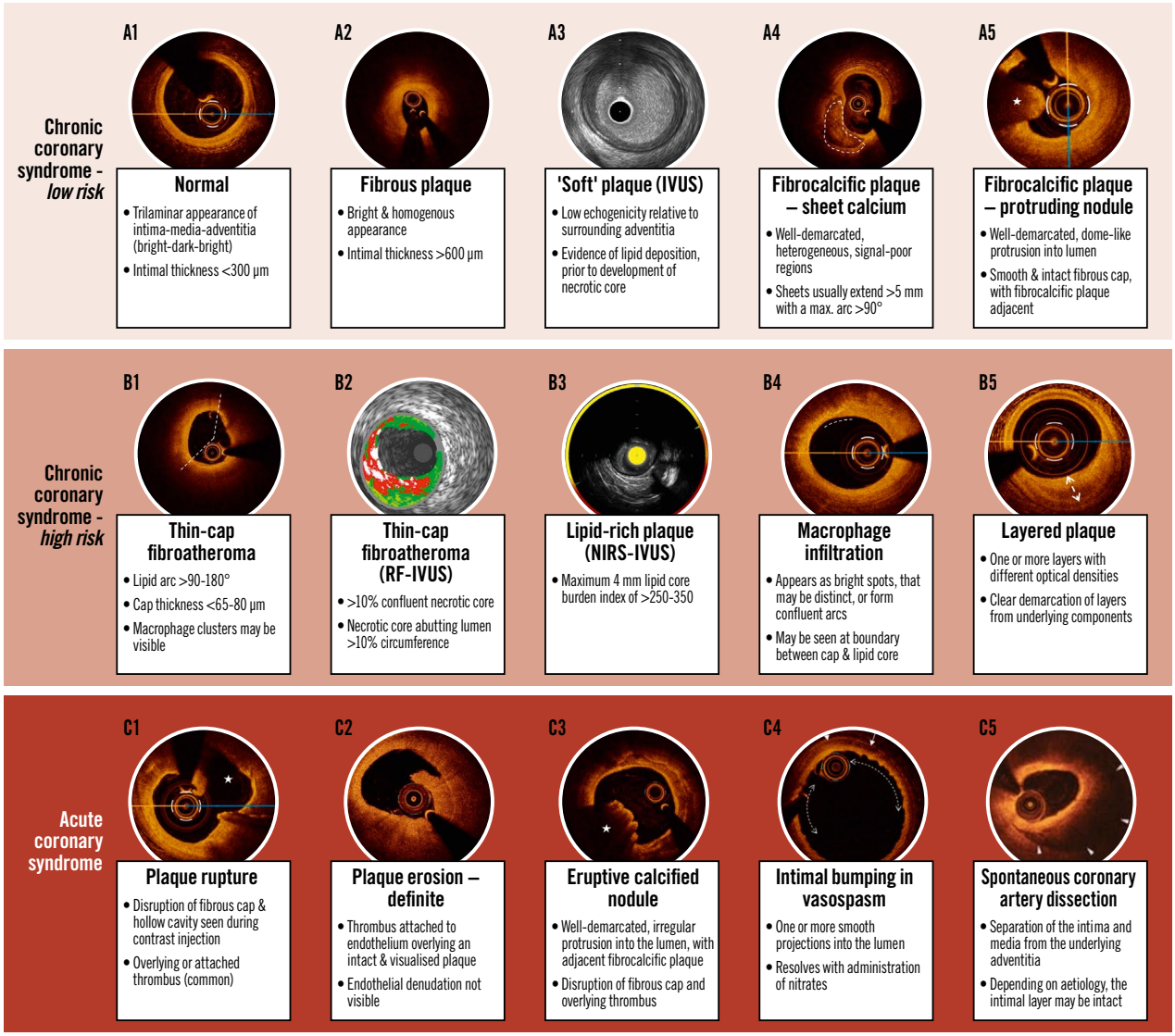

Michael McGarvey *et al.* • *EuroIntervention* 2026;22:e74-e89 • DOI: 10.4244/EIJ-D-25-00266

Reproduced with permission from[37,109,110]*. IVUS: intravascular ultrasound; NIRS: near-infrared spectroscopy; RF: radiofrequency*

increased risks of slow-reflow and periprocedural myocardial infarction (MI), and an IC imaging-guided strategy may favour pharmacological pretreatment and direct stenting[27,28].

Routine IC imaging assessment of patients with stent failure is essential to understand the underlying mode and mechanism of failure. IVUS can reliably quantify stent underexpansion, but OCT offers superior spatial resolution, enabling more accurate differentiation of thrombus from intimal hyperplasia, assessment of strut endothelialisation, identification of stent fracture, and differentiation of neointimal hyperplasia and neoatherosclerosis[29]. Several classification systems have been proposed to categorise stent failure and guide treatment according to findings seen on IC imaging **(Supplementary Table 2)**[29-31]. Whilst application of an IC imaging-guided approach to the management of stent failure is supported by expert consensus and observational data, further prospective trials are needed to confirm the impact of such an approach on clinical outcomes[32,33].

CULPRIT LESION IDENTIFICATION & TAILORED THERAPIES IN ACUTE SYNDROMES

In acute syndromes, contemporary IC imaging offers the potential to expand our understanding of the substrate, mechanisms, and manifestations of ACS *in vivo*. The link between plaque characteristics and ACS was initially established from post-mortem histological analysis of patients admitted with acute coronary thrombosis[24]. Fibroatheromas are plaques with a large lipid core and are categorised as

thin- or thick-cap according to the thickness of the overlying fibrous cap. In histological study, a cap thickness less than 65 µm is present in 95% of cases of plaque rupture (PR), and an inflammatory infiltrate is abundant in all cases of PR-associated thrombosis[24]. Whilst PR accounts for approximately half of ACS events, purely fibrous lesions may manifest as acute thrombosis due to plaque erosion (PE) with smooth muscle and endothelial cell loss at susceptible points in a plaque. Although the mechanism of this endothelial denudation remains unclear, PE is responsible for 30-40% of ACS[24]. This proportion appears to be increasing in the context of contemporary preventative therapy and mirrors a shifting prevalence of non-ST-segment elevation MI (NSTEMI) relative to ST-segment elevation MI (STEMI) in ACS presentation[5]. Lesions composed of dense collagen and sheet calcification (described as "fibrocalcific") are rarely associated with acute thrombosis, with ECNs causing fewer than 5% of acute events[24].

OCT permits characterisation of the underlying substrates of ACS due to atherosclerosis, the underlying mechanisms including PR and PE, and subsequent manifestations, such as white and red thrombi, with significantly greater sensitivity and reproducibility than IVUS[34]. OCT is therefore preferred for the assessment of patients admitted with ACS, particularly where the culprit lesion remains ambiguous despite coronary angiography[16]. One in five patients admitted with suspected MI have non-obstructed coronary arteries; using clinical, angiographic, and physiological criteria to identify the culprit lesion can result in inappropriate PCI in 25% of such patients[35,36]. OCT assessment enables identification of a culprit lesion in up to 50% of those with MI with non-obstructive coronary arteries, providing invaluable data to inform therapeutic decision-making[37].

OCT may identify other key diagnostic findings to guide management of patients following an acute presentation. Intimal bumping, representing folds in the intimal layer, is a pathognomonic finding of ACS secondary to coronary spasm **(Central illustration C4)**[37]. When spontaneous coronary artery dissection (SCAD) is suspected despite equivocal angiographic findings, intracoronary imaging may resolve diagnostic uncertainty, whilst acknowledging risks associated with instrumentation[16]. Expert opinion states that OCT may offer superior ability to discriminate SCAD from important differentials such as lipid-rich plaque **(Central illustration C5)**[38]. However, in one retrospective series of 63 patients with suspected SCAD assessed with OCT, complications were noted in five patients, including two cases of false lumen propagation[39]. In cases of suspected ACS secondary to microvascular or embolic aetiology, OCT facilitates the identification of a healthy, trilaminar vessel, increasing confidence in the diagnosis to guide further management.

Integrating a routine assessment of culprit lesions with high-resolution IC imaging may herald a new era of therapies tailored specifically to culprit lesion characteristics[5]. In the proof-of-concept EROSION study, a single-arm trial of 55 patients, a strategy of a purely antithrombotic treatment without PCI for OCT-adjudicated PE was associated with an acceptable major adverse cardiovascular events (MACE) rate of 7.5% at 1 year – whilst minimum lumen area (MLA) was unchanged, and nearly half of patients had no residual thrombus on 12-month OCT assessment[40]. EROSION III was a multicentre RCT of 246 patients with STEMI and restoration of flow, following vessel wiring or aspiration thrombectomy. Patients were randomised to OCT-guided or angiography-guided therapy. In the OCT-guided arm, two-thirds of patients had an underlying PR, whilst one-quarter had a PE. The investigators demonstrated that a physician-led strategy of OCT guidance was associated with less stent implantation (43.8% vs 58.8%; p=0.024) and equal MACE at 1 year (1.8% vs 2.6%; p=0.67) compared with an angiography-guided strategy[41]. Ongoing research in this area has the potential to shift ACS treatment to a mechanism-mediated approach, with routine characterisation of culprit arteries with IC imaging offering the potential to drive an important therapeutic shift.

Plaque composition, prognosis & automated lesion stratification

To date, IC imaging has been predominantly deployed as a tool for PCI planning and optimisation. This approach may limit the potential offered by IC imaging to refine lesion stratification, guide novel therapeutic approaches, and refine revascularisation decision-making.

PLAQUE MORPHOLOGICAL CHARACTERISTICS & RISK OF FUTURE EVENTS

IC imaging technologies have supported an evolution in our understanding of coronary atherosclerosis that may be reliably applied to inform lesion stratification and guide clinical care. Histological study established that a thin-cap fibroatheroma (TCFA), with evidence of cholesterol crystal deposition, a large necrotic core, neovascularisation, and immune cell infiltration, represents the highest clinical risk lesion and is commonly referred to as a "vulnerable" plaque[4,24].

Several IC imaging-based longitudinal cohort studies have confirmed these findings *in vivo* **(Supplementary Table 3)**[42-52]. In patients assessed with IVUS, a high plaque burden (>70%) is the strongest predictor of MACE, whilst an MLA ≤4.0 mm^2 and the presence of radiofrequency (RF)-IVUS-defined TCFA **(Central illustration B2)** are independent predictors of future MACE[42]. RF-IVUS applies spectral analysis to the IVUS backscatter signal to improve soft-tissue discrimination but does not significantly enhance the ability to identify lipid[53].

The addition of NIRS to IVUS can resolve this shortcoming. NIRS employs light in the infrared spectrum, at wavelengths of 700-1,000 nm, using a laser and sensor mounted on the imaging catheter to assess plaque composition and identify lipid with high precision[54]. The results are presented on a chemogram that maps the probability of a lipid core plaque onto a colour-coded graphical representation of the arterial wall, with yellow areas representing a >0.98 probability of the presence of lipid **(Central illustration B3)**. A numerical output termed the lipid core burden index (LCBI) is generated and, in the LRP study, an elevated maximum LCBI in any 4 mm segment of the scanned vessel (maxLCBI$_{4mm}$ [i.e., greater than 400]) carried a lesion-specific hazard ratio (HR) of 3.39 (95% confidence interval [CI]: 1.85-6.20)[46]. PROSPECT II demonstrated that a high plaque burden and large lipid core (i.e., plaque burden ≥70% and maxLCBI$_{4mm}$ ≥324.7) had a 4-year lesion-level MACE rate of 7.0%, compared with

0.2% when neither feature was present[47]. The combination of high-resolution IVUS with automated assessment of plaque lipid content enables identification of high-risk lesions in a manner that is both accessible and intuitive.

OCT can identify high-risk characteristics of vulnerable plaque with the greatest precision[55]. The CLIMA registry, of non-flow-limiting lesions in the left anterior descending artery (LAD), demonstrated that when each of the four cardinal features of high-risk plaque were present (i.e., MLA <3.5 mm^2, fibrous cap thickness <75 µm, lipid arc >180°, and OCT-defined macrophages), adverse events were predicted with an HR of 7.54 at 1 year (95% CI: 3.1-18.6)[48]. In the COMBINE OCT-FFR study, the presence of a TCFA in diabetic patients with non-flow-limiting lesions was associated with an almost 5-fold increase in the risk of cardiac death, target vessel MI, target lesion revascularisation, or hospitalisation with angina at 18 months (HR 4.65, 95% CI: 1.99-10.89)[49]. Following acute MI, non-culprit lesions with an MLA <3.5 mm^2 and a thin fibrous cap predicted an increased risk of MACE at 4 years, with an HR of 5.23 (95% CI: 2.98-9.17)[51].

Histological analysis and subsequent IC imaging studies *in vivo* suggest that many patients experience PR or PE events that are clinically silent, with acute thrombus formation followed by flow restoration and spontaneous healing. This subclinical process is associated with unstable syndromes and increased systemic risk[56]. Layered or healed coronary plaque may be best appreciated *in vivo* with OCT **(Central illustration B5)** and is associated with rapidly progressive lesions, multivessel disease, and increased atheroma burden[57]. In the COMBINE-OCT cohort, after TCFA, layered plaque was the strongest predictor of future adverse events[58]. It is likely that, as our understanding of vascular biology improves, the natural history of layered plaque, its role in plaque destabilisation and as a marker of underlying clinical risk will become more apparent.

THE MORPHOFUNCTIONAL ASSESSMENT – A NOVEL APPROACH TO INVASIVE LESION ASSESSMENT

Important barriers to widespread adoption of IC imaging, particularly for advanced lesion stratification and ACS culprit identification, include challenges with image interpretation, duration of image analysis in routine practice, and reproducibility between operators[6]. Applying AI techniques to IC imaging interpretation has the potential to address many of these concerns, with novel technologies enabling automated image segmentation and three-dimensional computational reconstruction, from which lumen contours, arterial dimensions, and atherosclerotic plaque composition can be modelled[59]. Such models are increasingly integrated into proprietary vendor-provided and dedicated bespoke software for both IVUS and OCT[59-63].

AUTOMATED PLAQUE ANALYSIS

Automated plaque characterisation has evolved in complexity and performance with expansion in AI techniques and computational power. Early iterations focused on identification and quantification of calcium, with a discriminatory accuracy of 0.91-0.99 in published datasets[64]. Calcium detection algorithms are now integrated into commercially available software but lack prospective clinical validation. Algorithms for identification of fibrous and lipid-rich plaque demonstrate high degrees of accuracy in derivation and external validation cohorts but require further validation prior to integration into routine practice. Lipid-rich plaque may be further characterised with assessment of fibrous cap thickness, lipid angle, cholesterol crystal and macrophage infiltration within 25 seconds of image acquisition[59,65-67]. We may now be approaching an era where identification of high-risk or vulnerable plaque can be performed in routine care to improve lesion stratification and direct therapy.

In acute syndromes, whilst plaque rupture can often be readily identified, plaque erosion is a diagnosis of exclusion *in vivo*, as even OCT lacks the requisite spatial resolution **(Central illustration C1, C2)**. Recently described deep-learning (DL) algorithms enable identification and quantification of luminal thrombus[68] and enhance diagnosis of plaque erosion so that even inexperienced operators may operate at the level of an expert clinician[69]. Whilst an exciting demonstration of the potential of AI, these models remain in an early stage of development.

IMAGING-DERIVED FRACTIONAL FLOW RESERVE

In patients with CCS undergoing invasive angiography, international guidelines currently recommend with a Class I, Level of Evidence A recommendation that intermediate stenoses should undergo invasive functional stratification using fractional flow reserve (FFR) or the instantaneous wave-free ratio (iFR)[2]. In the FAME study, revascularisation guided by FFR enabled safe deferral of PCI, with reductions in death, non-fatal MI, and revascularisation at 1 year[70]. FAME II showed that in "functionally significant" lesions, pressure-wire guided PCI was associated with a reduction in urgent symptom-guided revascularisation but no difference in prognostically relevant events such as spontaneous MI or death[71]. The magnitude of abnormality on FFR/iFR is associated with the burden of "typical" or "Rose" angina[72], whilst a higher pullback pressure gradient (PPG; i.e., >0.66) identifies focal lesions where PCI is most likely to deliver a symptomatic benefit[73].

A lesion's functional behaviour is intrinsically linked to its morphological characteristics. Lipid-rich plaque, as assessed by RF-IVUS, is correlated with a reduced FFR, with a concomitant reduction in FFR as the size of the necrotic core increases[74]. Focal lesions with an FFR <0.80 and a raised PPG demonstrate increased plaque volume, a large lipid burden, and a higher prevalence of TCFA than diffuse lesions[75] **(Figure 1)**.

Automated image interpretation using AI, paired with advances in fluid dynamic modelling, may now combine these two concepts and enable a comprehensive morphofunctional assessment using a single IC imaging device. This has the potential to transform cardiac catheterisation laboratory workflows and render the functional versus morphological dichotomy redundant[76]. Automated lumen contouring permits the generation of a physiological model from which "functional" significance may be predicted. IVUS- and OCT-derived FFR models have been reported, with both demonstrating good correlation with wire-based FFR. Such calculations are increasingly performed in under 1 minute, sufficient to guide real-time clinical decision-making. OCT-based FFR (OFR) combines a model of virtual hyperaemic

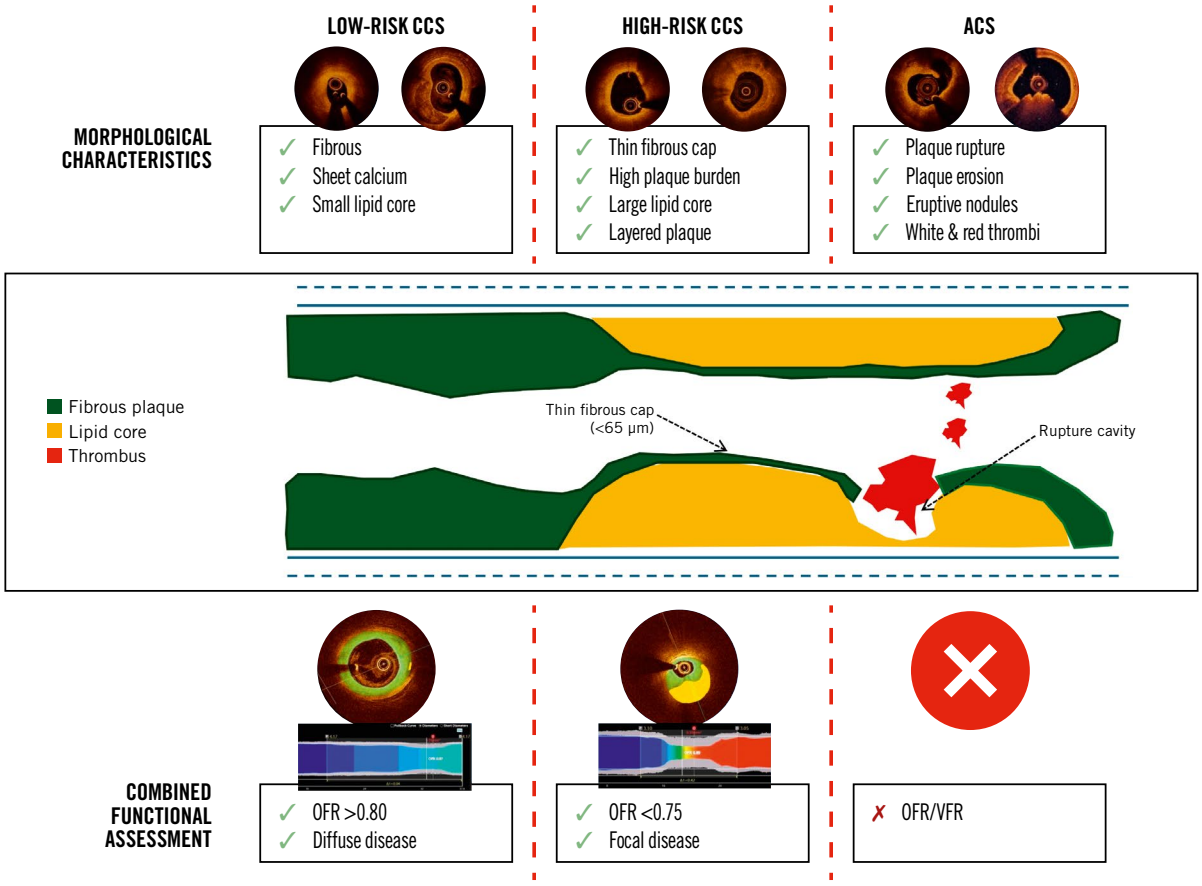

Figure 1. *Morphofunctional lesion stratification with AI-enabled intracoronary imaging. ACS: acute coronary syndrome; AI: artificial intelligence; CCS: chronic coronary syndrome; OFR: optical coherence tomography-based fractional flow reserve; VFR: virtual flow reserve*

flow velocity with automated lumen contouring to generate an OFR pullback, with the distal value corresponding to invasive FFR. Computation can be performed in 55 seconds on a standard laptop after importing OCT digital imaging and communications in medicine (DICOM) images and identified physiologically significant stenoses (i.e., wire-based FFR ≤0.80) with an area under the curve (AUC) of 0.93 (95% CI: 0.87-0.97). Performance was similar in LAD and non-LAD lesions and outperformed the optimal MLA threshold (1.89 mm^2), which had an AUC of 0.80 (95% CI: 0.72-0.86)[77]. Virtual flow reserve (VFR) uses an alternative, lumped-parameter model based on OCT-derived lumen geometry to estimate functional significance. Rather than estimating coronary flow or microvascular function, VFR is based on model-derived pressure losses to produce an estimate of wire-based FFR. This can be computed during OCT acquisition, adding less than 1 second. In a validation study, this showed good correlation with wire-based FFR, predicting flow-limiting stenoses with an AUC of 0.88 (95% CI: 0.84-0.92)[78].

POST-PCI ASSESSMENT

IC imaging vendor software now provides measures of absolute and relative stent expansion that are increasingly complex but superior to conventional measures – the volumetric stent expansion index, for example, significantly outperforms MSA as a predictor of future events[79]. The application of a combined morphofunctional assessment may identify patients with a well-expanded stent and an optimal functional result, free of post-PCI complications. Such patients may benefit from early de-escalation of antianginal and dual antiplatelet therapies (DAPT). Conversely, early identification of those at greatest risk of target vessel failure may guide physicians towards escalated preventative therapy and extended DAPT[80]. We are on the cusp of an era where we can characterise the heterogeneity of atherosclerotic plaque, its functional and anatomical profile, and the success of PCI, all with IC imaging and AI-enabled software[81]. Whilst highly promising, these technologies remain expensive, and recent data assessing the accuracy of angiography-derived functional assessment highlight the importance of prospective clinical validation prior to widespread application[82].

Preventative therapy for high-risk plaque

The association between lesion morphological features and clinical outcome has focused attention on targeted therapies to ameliorate risk. Treatment strategies may be categorised as mechanical, systemic pharmacological therapy or local therapy to promote plaque pacification **(Table 2)**[41,83-90].

Table 2. Targeted therapies for patients with high-risk lesions as assessed with intracoronary imaging.

Study	Cohort	Comparison	Primary endpoint	Results	High-risk lesion criteria
IC imaging-guided local therapy for high-risk plaque					
PREVENT (2024)[83]	1,606 patients CCS & non-culprit ACS Non-flow-limiting lesions (FFR >0.80) High-risk lesion as per IC imaging criteria	Medical therapy vs PCI with DES or BVS 1:1 randomisation	Primary endpoint: Composite of cardiac death, target vessel MI, ischaemia-driven TVR, or hospitalisation with progressive or unstable angina	Primary endpoint: 3.4% OMT vs 0.4% PCI at 2 yrs (p=0.0003) 33% of patients in PCI arm treated with BVS 100% of PCI were optimised using IC imaging	At least 2 of the following: MLA <4.0 mm^2 by IVUS or <3.5 mm^2 by OCT Plaque burden >70% (by IVUS) TCFA (according to RF-IVUS* or OCT criteria#) Lipid-rich plaque (maxLCBI$_{4mm}$ >315)
DEBuT-LRP (2024)[84]	20 patients Non-culprit lesions in NSTE-ACS Non-flow-limiting with lipid-rich plaque	Baseline vs 9-month follow-up maxLCBI$_{4mm}$ following treatment with paclitaxel DCB	Primary endpoint: Change in maxLCBI$_{4mm}$ from baseline	Primary endpoint: Baseline maxLCBI$_{4mm}$ 397 (IQR 299-597) vs 9-month maxLCBI$_{4mm}$ 211 (IQR 106-349) (p<0.001)	Lipid-rich plaque, as assessed by NIRS-IVUS: Any lesion with maxLCBI$_{4mm}$ >325
PROSPECT ABSORB (2020)[85]	182 patients Non-culprit lesions in ACS Non-flow-limiting lesions (FFR >0.80, iFR >0.89) Plaque burden ≥65%, as assessed by IVUS Suitable for BVS	Medical therapy vs PCI with BVS 1:1 randomisation	Primary endpoint: Minimum lumen area on follow-up IVUS Secondary safety endpoint: Composite of cardiac death, target vessel MI, or clinically driven TLR	Primary endpoint: 3.0±1.0 mm^2 OMT vs 6.9±2.6 mm^2 BVS at 2 yrs (p≤0.0001) Secondary safety endpoint: 4.5% OMT vs 4.3% BVS at 2 yrs	As assessed by NIRS-IVUS: Plaque burden ≥70% MLA ≤4.0 mm^2 MaxLCBI$_{4mm}$ ≥324.7 95% of lesions had ≥1 high-risk characteristic 74% of lesions had ≥2 high-risk characteristics 43% had all 3 high-risk characteristics
PECTUS (2020)[86]	34 patients (planned for 500 but terminated early) Non-culprit lesions in ACS Non-flow-limiting lesions (FFR ≥0.80) OCT-defined vulnerable plaque suitable for BVS	Medical therapy vs PCI with BVS 1:1 randomisation	Primary endpoint: Composite of all-cause mortality, non-fatal MI, and unplanned TVR	Primary endpoint: 1 event OMT vs 3 events BVS at 2 years	Any 2 of the following (as assessed by OCT): Lipid arc >90° Cap thickness <65 µm OCT-defined cap rupture or thrombus formation
FORZA (2020)[87]	350 patients CCS & non-culprit lesions in ACS Angiographically intermediate stenosis (30-80%)	FFR-guided PCI with DES vs OCT-guided PCI with DES 1:1 randomisation	Primary endpoint: Composite of death, MI, target vessel revascularisation and significant residual angina (SAQ <90)	Primary endpoint: 14.8% FFR guidance vs 8.0% OCT guidance (p=0.048) 32% of FFR arm treated with PCI vs 53% of OCT arm	One of the following (as assessed by OCT): Area stenosis ≥75% Area stenosis >50% but <75% and MLA <2.5 mm^2 Area stenosis >50% but <75% and plaque rupture
EROSION III (2022)[41]	246 patients STEMI & TIMI III flow and <70% residual stenosis after wiring +/– thrombectomy Conservative stenting strategy with DES placement in high-risk lesions only	Angiography-guided primary PCI vs OCT-guided primary PCI 1:1 randomisation	Primary endpoint: Rate of DES placement Primary safety endpoint: Composite of cardiac death, recurrent MI, TLR, and hospitalisation with unstable angina at 1 month Secondary safety endpoint: Composite of cardiac death, recurrent MI, TLR, and hospitalisation with unstable angina at 1 year	Primary endpoint: 44.8% DES placement with angio-guided PCI vs 58.8% with OCT guidance (p=0.032) Primary safety endpoint: 3 events with angio guidance vs 2 events with OCT guidance at 1 month (p=0.67) Secondary safety endpoint: 10 events with angio guidance vs 11 events with OCT guidance	High-risk ACS lesion (as assessed by OCT): Plaque rupture with dissection and/or haematoma Conservative stenting strategy advised if OCT-defined ACS mechanism was: Plaque erosion Plaque rupture without dissection and/or haematoma Spontaneous coronary artery dissection
IC imaging-guided systemic therapy for high-risk plaque					
COLOCT (2024)[88]	128 patients Non-culprit lesions in ACS Angiographically intermediate stenosis (30-70%) OCT-defined lipid-rich plaque	Placebo vs 0.5 mg colchicine daily 1:1 randomisation	Primary endpoint: Change in minimal fibrous cap thickness at 1 year Secondary safety endpoint: Composite of all-cause death, non-fatal MI, non-fatal stroke, and ischaemia-driven revascularisation at 1 year	Primary endpoint: +51.9 µm (IQR 32.8-71.0) with placebo vs +87.2 µm (IQR 69.9-104.5) with colchicine (p=0.006) Secondary safety endpoint: 17.3% of participants with placebo vs 11.5% with colchicine (p=0.402)	Lipid-rich plaque, as assessed by OCT: Lipid arc >90°
COCOMO-ACS (2024)[89]	64 patients Non-culprit lesions in NSTE-ACS Angiographically intermediate stenosis (20-50%) OCT-defined lipid-rich plaque	Placebo vs 0.5 mg colchicine daily 1:1 randomisation	Primary endpoint: Change in minimal fibrous cap thickness at 12-18-month follow-up Secondary safety endpoint: Composite of death, non-fatal MI, non-fatal stroke or TIA, repeat revascularisation, or unplanned hospitalisation 12-18-month follow-up	Primary endpoint: +29.4±19.7 µm with placebo vs +39.0±20.3 µm with colchicine (p=0.08) Secondary safety endpoint: 10 events with placebo vs 7 events with colchicine	Lipid-rich plaque, as assessed by OCT: Lipid arc >90° Fibrous cap thickness ≤120 µm
YELLOW III (2023)[90]	110 patients CCS patients Angiographically intermediate stenosis (30-50%) OCT features of lipid-rich plaque	Baseline vs 6-month follow-up fibrous cap thickness and maxLCBI$_{4mm}$ following treatment with evolocumab	Co-primary endpoint: Change in minimal fibrous cap thickness & maxLCBI$_{4mm}$ at 6-month follow-up	Co-primary endpoint: Fibrous cap thickness: Baseline 70.9±21.7 µm vs 6-month 97.7±31.1 µm (p<0.001) MaxLCBI$_{4mm}$: Baseline 306.8±177.6 vs 6-month 213.1±168.0 (p<0.001)	OCT-defined lipid-rich plaque requires: Lipid arc >90° Fibrous cap thickness ≤120 µm

Table 2. Targeted therapies for patients with high-risk lesions as assessed with intracoronary imaging (cont'd).

Study	Cohort	Comparison	Primary endpoint	Results	High-risk lesion criteria
Ongoing trials of IC imaging-guided therapy for high-risk plaque					
INTERCLIMA (NCT05027984)	1,420 patients (estimated) Non-culprit lesions in ACS Angiographically intermediate lesion (40-70% stenosis)	FFR/iFR-guided PCI vs OCT-guided PCI Perform OCT-guided PCI if features of vulnerable plaque	Primary endpoint: Composite of cardiac death or non-fatal target vessel MI	Awaited 2025	OCT-defined vulnerable plaque requires fibrous cap thickness <75 µm and 2 of the following: MLA <3.5 mm^2 Lipid arc >180° Macrophage infiltration
COMBINE-INTERVENE (NCT05333068)	1,222 patients (estimated), with *de novo* multivessel disease (i.e., ≥2 *de novo* lesions in 2 native arteries) ACS or CCS presentation Eligible lesions may be culprit ACS lesions, or target lesion with >50% stenosis and TIMI III flow in >2 mm vessel	FFR-guided PCI vs combined FFR-OCT guidance 1:1 randomisation Perform PCI in combined guidance if: FFR ≤0.75 and Vulnerable plaque on OCT	Primary endpoint: Composite of cardiac death, any MI, or any clinically driven revascularisation	Awaited 2026	OCT-defined vulnerable plaque requires 1 of the following: TCFA (cap thickness ≤75 µm) Ruptured plaque Plaque erosion with 70% area stenosis or MLA <2.5 mm^2
VULNERABLE (NCT05599061)	600 patients (estimated) Non-culprit lesions following STEMI Angiographically intermediate lesion (40-69%) Non-flow-limiting, with FFR >0.80 OCT features of vulnerable plaque	OMT vs OCT-guided PCI of vulnerable plaque 1:1 randomisation	Primary endpoint: Composite of cardiovascular death, target vessel MI, clinically or physiologically guided TVR	Awaited 2028	OCT-defined vulnerable plaque requires all 3 features: Lipid arc >90° for 5 mm length Fibrous cap thickness ≤80 µm OCT-defined plaque burden ≥70% Plaque burden calculated as: [(max.EEM reference area - MLA)/ max. EEM reference area]*100
ESCALATE (NCT06469528)	50 patients (estimated) CCS patients with hs-CRP ≥2.0 Angiographically intermediate lesions (30-80%) Non-flow-limiting (FFR >0.80) OCT features of high-risk plaque	OMT vs 0.5 mg colchicine daily 1:1 randomisation	Primary endpoint: Change in minimal fibrous cap thickness at 6-month follow-up	Awaited 2027	OCT-defined high-risk plaque requires: Lipid arc >90° Fibrous cap thickness ≤120 µm

*RF-IVUS defined TCFA: ≥10% confluent necrotic core with >30° abutting the lumen in three consecutive frames. #OCT defined TCFA: a lipid plaque with arc >90° and fibrous cap thickness <65 µm. ACS: acute coronary syndrome; BVS: bioabsorbable vascular scaffold; CCS: chronic coronary syndrome; DCB: drug-coated balloon; DES: drug-eluting stent; EEM: external elastic membrane; FFR: fractional flow reserve; hs-CRP: high-sensitivity C-reactive protein; IC: intracoronary; iFR: instantaneous wave-free ratio; IQR: interquartile range; IVUS: intravascular ultrasound; maxLCBI$_{4mm}$: maximal lipid core burden indexed in a 4 mm segment; MI: myocardial infarction; MLA: minimum lumen area; NIRS: near-infrared spectroscopy; NSTE-ACS: non-ST-segment elevation acute coronary syndrome; OCT: optical coherence tomography; OMT: optimal medical therapy; PCI: percutaneous coronary intervention; RF: radiofrequency; SAQ: Seattle Angina Questionnaire; STEMI: ST-segment elevation myocardial infarction; TCFA: thin-cap fibroatheroma; TIA: transient ischaemic attack; TIMI: Thrombolysis in Myocardial Infarction; TLR: target lesion revascularisation; TVR: target vessel revascularisation

TARGETED MECHANICAL THERAPY

The FORZA trial tested a morphology-based stratification against traditional physiological testing. A total of 350 patients with angiographically moderate lesions were randomised to an OCT assessment versus FFR. Patients randomised to the OCT arm (with either chronic or acute coronary syndromes) underwent PCI if there was an area stenosis (AS) ≥75% or if there was an AS ≥50% but <75% and evidence of plaque rupture or MLA <2.5 mm^2. At 13 months, the composite outcome of significant angina and all-cause MACE was significantly reduced in the OCT arm[87]. The FLAVOUR trial applied an IVUS-guided approach, comparing an MLA threshold <3 mm^2 (or 3-4 mm^2 with a plaque burden >70%), versus FFR-guided revascularisation and demonstrated non-inferiority in terms of MACE at 2 years[91]. In a blinded *post hoc* analysis, post-PCI physiological assessment was an independent predictor of target vessel failure at 2 years, with this finding most marked in the IVUS-guided group. This further supports the importance of a combined morphofunctional assessment in PCI optimisation[92].

The PREVENT Trial tested a morphology-led approach to lesion stratification in angiographically moderate, non-culprit lesions deemed suitable for medical management (i.e., FFR >0.80). A total of 5,627 patients were assessed with IC imaging, and high-risk features (either by IVUS, RF-IVUS, NIRS-IVUS or OCT criteria) were present in 1,606 individuals who were randomised to IC imaging-guided PCI or optimal medical therapy. At 2 years, there was a 3% absolute reduction in the primary composite outcome, predominantly driven by reductions in hospitalisation with angina and target vessel revascularisation (TVR). The incidence of TVR in the IC imaging-guided PCI arm was just 1.7% at 4 years[83]. One-third of patients in the intervention arm in PREVENT were treated with bioabsorbable scaffolds, with the results reflecting those of the prematurely terminated PROSPECT ABSORB study[85].

There are three ongoing clinical outcome trials testing a morphology-based approach: The VULNERABLE Trial (ClinicalTrials.gov: NCT05599061) will randomise 2,500 patients admitted with STEMI and FFR-negative non-culprit lesions with high-risk features on OCT to PCI versus medical therapy; INTERCLIMA (NCT05027984) will test a functional versus morphological assessment with OCT to guide revascularisation decisions in angiographically moderate, non-culprit lesions in patients with ACS; and COMBINE-INTERVENE (NCT05333068) will test a combined assessment with FFR/OCT versus FFR alone

in all-comers, regardless of their clinical syndrome, with angiographically moderate lesions. Whilst testing a similar hypothesis, these trials have applied different IC imaging selection criteria, which will be an important consideration **(Figure 2)**.

LOCAL THERAPIES FOR PLAQUE STABILISATION

Due to concerns related to permanent device placement in preventative intervention and the high number needed to treat in the PREVENT study (i.e., ~150 PCIs to prevent 1 target vessel MI at 2 years), there remains significant interest in alternative locally applied therapy. The DEBuT-LRP pilot study assessed the role of drug-coated balloons (DCBs) for preventative PCI in high-risk lipid-rich lesions, as assessed with NIRS-IVUS. At 9 months, but not at baseline, treatment with paclitaxel DCBs caused significant reductions in lipid-core burden, with no intervention-related complications[84]. The targeted application of cryotherapy to high-risk lesions promotes lesion stabilisation in preclinical models[93], and results from the POLARSTAR first-in-human study are awaited (ClinicalTrials.gov: NCT05600088). It is likely that there will be an expansion in studies evaluating the role of local therapies for high-risk plaques, where it will be important to show improvement in outcomes when tested against current standard of care.

PHARMACOLOGICAL APPROACHES TO HIGH-RISK PLAQUE

Coronary atherosclerotic plaque is highly dynamic, and its activity is partly related to the presence and control of established cardiovascular risk factors[94]. Multiple intracoronary imaging outcome trials have demonstrated the plaque-stabilising effects of lipid-modifying therapies[4], with high-intensity statin therapy[95] and PCSK9 inhibition being the most intensively studied[96]. In these large prospective clinical studies, reductions in plasma low-density lipoprotein consistently led to reductions in plaque atheroma volume and plaque lipid content (as measured with $LCBI_{4mm}$ and maximal lipid arc) and increases in fibrous cap thickness – patients who exhibited improvement in all three features ("triple regression") demonstrated a significant reduction in adverse events at 1 year[97].

Multiple randomised clinical trials have established the beneficial effects of anti-inflammatory therapy in patients with recent or historical myocardial infarction[98]. A single-centre OCT study has provided biological plausibility for these findings, as treatment with colchicine increased

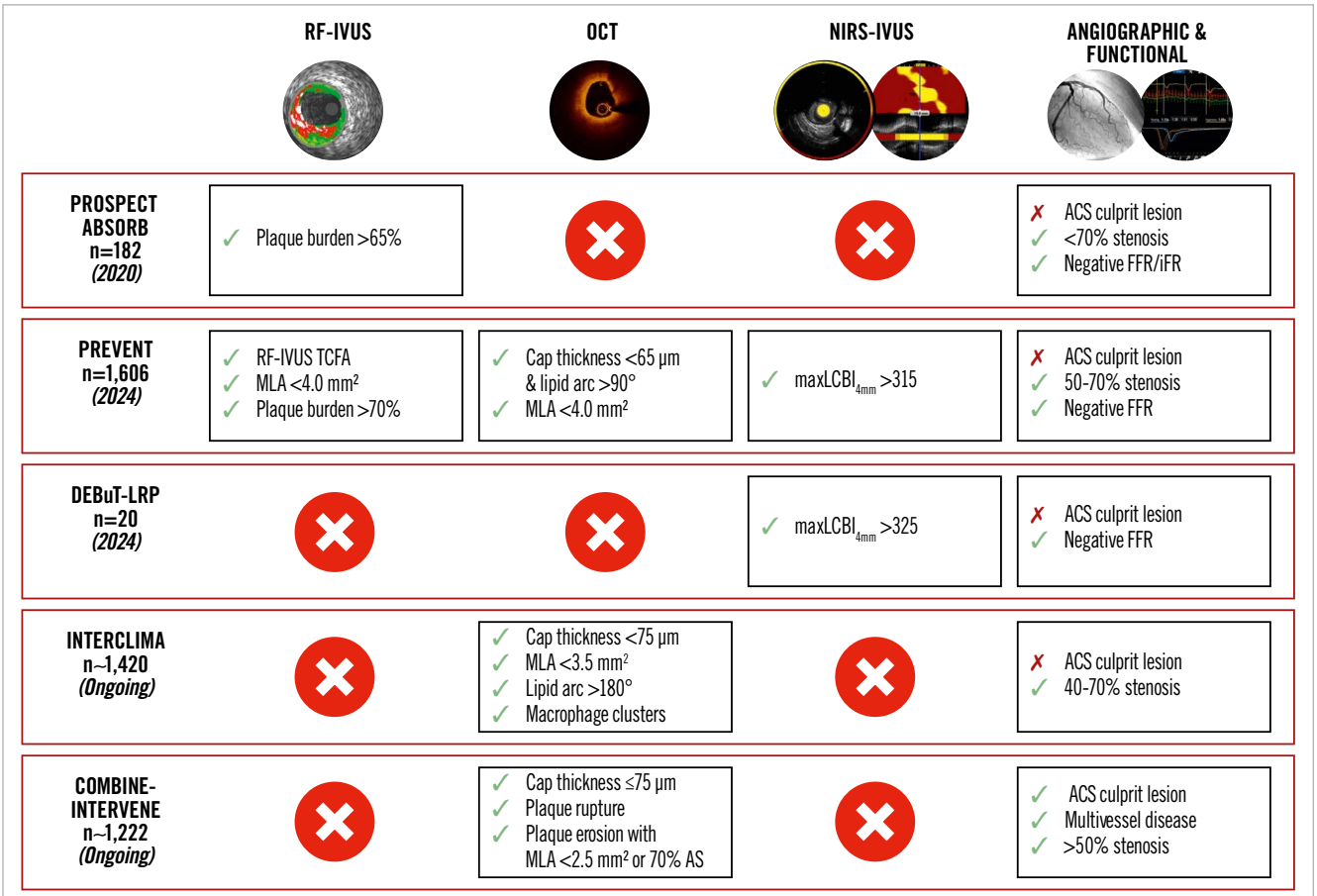

Figure 2. *Lesion stratification in clinical trials assessing device-based therapy for high-risk plaque. ACS: acute coronary syndrome; AS: aortic stenosis; FFR: fractional flow reserve; iFR: instantaneous wave-free ratio; IVUS: intravascular ultrasound; $maxLCBI_{4mm}$: maximum lipid core burden index in any 4 mm segment; MLA: minimum lumen area; NIRS: near-infrared spectroscopy; OCT: optical coherence tomography; RF: radiofrequency; TCFA: thin-cap fibroatheroma*

fibrous cap thickness whilst reducing maximal lipid arc and macrophage infiltration[88]. As the armamentarium of disease-modifying therapy expands, stratification with IC imaging has the potential to direct escalated medical therapy to those patients likely to benefit most.

Future directions & novel technologies

NOVEL PROGNOSTIC INDICATORS

As AI models for automated lesion assessment develop and evolve, new imaging biomarkers of patient risk will emerge. OCT-derived lipid core burden index is one example of a novel quantitative marker of lesion lipid components that has been validated against NIRS-IVUS[99]. An OCT-derived $maxLCBI_{4mm}$ >400 predicted increased risks of cardiac death, MI, and target vessel revascularisation with a hazard ratio of 1.87, whilst lesions with a $maxLCBI_{4mm}$ >400 and a thin fibrous cap carried a hazard ratio of 4.87 compared to lesions where neither feature was present[100]. The lipid-to-cap ratio (LCR) is another novel marker of risk that can be computed simultaneously with a functional assessment with OFR. In a study of 915 non-culprit lesions in patients admitted with ACS, a low OFR and a high LCR predicted 2-year vessel-related MI and revascularisation with a hazard ratio of 15.19 (95% CI: 5.82-39.63), highlighting the potential of this novel and automated morphofunctional approach to stratification[101].

Morphofunctional assessment currently relies on models of coronary flow and pressure loss that are derived solely from cross-sectional imaging. A recently described Doppler OCT catheter, however, would enable direct measurement of coronary blood flow in real-time alongside cross-sectional imaging. This offers the potential to enhance the reliability of functional assessment of epicardial stenoses, to integrate microvascular assessment, and to deliver a truly comprehensive assessment to guide lesion stratification[102].

INCORPORATING PLAQUE BIOMECHANICS

Alongside plaque anatomical and functional characteristics, assessment of plaque biomechanics may enhance lesion stratification. Low endothelial shear stress has long been acknowledged as a predictor of rapid lesion progression and increased clinical risk, but translation into clinical practice has proved challenging[103]. These calculations can now be rapidly and reliably performed using AI analysis of IC imaging, though they are not yet available commercially[104]. This will facilitate assessment of increasingly granular indices of plaque biomechanics, such as endothelial shear stress gradient and plaque structural stress, which are independent markers of risk when assessed alongside established anatomical markers of high-risk plaque and predictors of future or recurrent ACS[105].

MULTIMODALITY DEVICES & PLAQUE "THERANOSTICS"

NIRS-IVUS is the first multimodality device to be introduced to routine clinical practice, but there is now a growing armamentarium of dual or multimodality catheters. The HyperVue Imaging System (SpectraWAVE) pairs "deep" OCT imaging (DeepOCT [SpectraWAVE]) with NIRS lipid detection to enhance detection of the key features of high-risk plaque – DeepOCT enables quantification of plaque burden and fibrous cap thickness, detection of immune cell infiltration, and assessment of lipid core burden with NIRS analysis[106]. Combining IVUS or OCT with novel light-based imaging modalities allows detailed characterisation of plaque metabolic properties, in addition to morphological characteristics. Intravascular photoacoustic imaging provides assessment of endothelial integrity, macrophage colocation and cell-adhesion molecule expression, whilst catheters that detect near-infrared autofluorescence detect oxidative stress resulting from lipoprotein oxidation and intraplaque haemorrhage[107].

Such devices may facilitate the ongoing evolution of IC imaging from a tool used to optimise intervention and refine lesion stratification into a tool to enable delivery of targeted therapy. Near-infrared fluorescence (NIRF) molecular imaging requires the infusion of activatable tracers that bind to molecules within metabolically active atherosclerotic plaque and fluoresce when excited with near-infrared light. In a rabbit model of atherosclerosis, a highly inflamed atherosclerotic lesion (characterised by a high NIRF signal) was identified – a NIRF-emitting, photoactivatable agent targeted to macrophages was infused and photoactivated using near-infrared light from the imaging catheter. This resulted in activation of the drug molecule, subsequent attenuation of macrophage activity, resolution of inflammation, and transition from a high-risk lipid-rich plaque to a predominantly fibrous morphology, as assessed by OCT[108]. This combined "theranostic" approach highlights the central role that IC imaging has potential to play in the assessment, stratification, and treatment of patients with clinically significant coronary atherosclerosis.

Conclusions

IC imaging-guided PCI leads to reductions in target vessel MI, lesion revascularisation, cardiac death, and all-cause death, when compared to angiography-guided interventions, and should now be viewed as the standard of care in patients with high clinical or anatomical complexity. IC imaging has the potential to transform how we understand and manage patients with CAD, offering personalised percutaneous and pharmacological therapies. Routine characterisation of lesion characteristics may be used to improve patient stratification and refine treatment within and beyond the catheterisation laboratory for both chronic and acute coronary syndromes. Automated image interpretation using AI, with integrated morphofunctional assessment, has the potential to democratise expertise and support a step change in interventional cardiology as we move towards targeted application of an ever-larger armamentarium of mechanical and pharmacological interventions.

Authors' affiliations

1. Department of Cardiology, King's College Hospital NHS Foundation Trust, London, United Kingdom; 2. BHF Centre of Excellence, School of Cardiovascular and Metabolic Medicine & Sciences, King's College London, London, United Kingdom; 3. Department of Cardiology, Guy's & St Thomas' NHS Foundation Trust, London, United Kingdom; 4. Essex Cardiothoracic Centre, Mid and South Essex NHS Foundation

Trust, Basildon, United Kingdom; 5. Anglia Ruskin University, School of Medicine & Medical Technology Research Centre, Chelmsford, United Kingdom; 6. Bristol Heart Institute, University Hospitals Bristol NHS FT & University of Bristol, Bristol, United Kingdom; 7. Department of Cardiology, University Hospitals of Dorset NHS Foundation Trust, Bournemouth, United Kingdom; 8. Department of Cardiology, St. Francis Hospital, Roslyn, NY, USA; 9. New York Institute of Technology, Old Westbury, NY, USA; 10. School of Biomedical Engineering, Shanghai Jiao Tong University, Shanghai, China; 11. Department of Cardiology, Erasmus MC, Rotterdam, the Netherlands; 12. Department of Cardiology, Royal Free NHS Foundation Trust, London, United Kingdom; 13. Department of Cardiology, Royal Brompton & Harefield Hospitals, Guy's & St Thomas' NHS Foundation Trust, London, United Kingdom; 14. 1st Department of Cardiology, Medical University of Gdańsk, Gdańsk, Poland

Funding

This work was supported by the British Heart Foundation Centre of Research Excellence (Grant no. RE/24/130035). N. Pareek is supported by the Margaret Sail Novel Emerging Technology grant from Heart Research UK (RG2693).

Conflict of interest statement

M. McGarvey: research grant from Abbott. K. De Silva: speaker honoraria from Abbott, Boston Scientific, Medtronic, Philips, and Shockwave Medical. T.R. Keeble: advisory board member and research grants with Abbott and Philips; and speaker fees from Nipro. T.W. Johnson: institutional research grants from Abbott; and consultancy/speaker fees from Abbott, Boston Scientific, Cordis, Medtronic, and Terumo. P. O'Kane: speaker fees from Abbott. Z.A. Ali: institutional grant support from Abbott, Abiomed, ACIST Medical, Amgen, Boston Scientific, CathWorks, Canon, Conavi, HeartFlow, Inari Medical, Medtronic, National Institute of Health, Nipro, Opsens Medical, Medis, Philips, Shockwave Medical, Siemens, SpectraWAVE, and Teleflex; consulting fees from Abiomed, AstraZeneca, Boston Scientific, CathWorks, Opsens Medical, Philips, and Shockwave Medical; and equity in Elucid, Lifelink, SpectraWAVE, Shockwave Medical, and VitalConnect. S. Tu: co-founder of Pulse Medical; research grants and consultancy from Pulse Medical. J.M. Hill: speaker honoraria and institutional grants from Abbott, Abiomed, Boston Scientific, and Shockwave Medical; has received equity from Shockwave Medical; and consultancy fees from SpectraWAVE. R. Dworakowski: speaker honoraria and proctor fees from Abbott. N. Pareek: honoraria and educational grants from Abbott Vascular, honoraria from NIPRO; and serves on the Advisory Boards for Boston Scientific and Johnson & Johnson. The other authors have no conflicts of interest to declare.

References

1. Stone GW, Christiansen EH, Ali ZA, Andreasen LN, Maehara A, Ahmad Y, Landmesser U, Holm NR. Intravascular imaging-guided coronary drug-eluting stent implantation: an updated network meta-analysis. *Lancet*. 2024;403:824-37.

2. Vrints C, Andreotti F, Koskinas KC, Rossello X, Adamo M, Ainslie J, Banning AP, Budaj A, Buechel RR, Chiariello GA, Chieffo A, Christodorescu RM, Deaton C, Doenst T, Jones HW, Kunadian V, Mehilli J, Milojevic M, Piek JJ, Pugliese F, Rubboli A, Semb AG, Senior R, Ten Berg JM, Van Belle E, Van Craenenbroeck EM, Vidal-Perez R, Winther S; ESC Scientific Document Group. 2024 ESC Guidelines for the management of chronic coronary syndromes. *Eur Heart J*. 2024;45:3415-537.

3. Rao SV, O'Donoghue ML, Ruel M, Rab T, Tamis-Holland JE, Alexander JH, Baber U, Baker H, Cohen MG, Cruz-Ruiz M, Davis LL, de Lemos JA, DeWald TA, Elgendy IY, Feldman DN, Goyal A, Isiadinso I, Menon V, Morrow DA, Mukherjee D, Platz E, Promes SB, Sandner S, Sandoval Y, Schunder R, Shah B, Stopyra JP, Talbot AW, Taub PR, Williams MS. 2025 ACC/AHA/ACEP/NAEMSP/SCAI Guideline for the Management of Patients With Acute Coronary Syndromes: A Report of the American College of Cardiology/American Heart Association Joint Committee on Clinical Practice Guidelines. *Circulation*. 2025;151:e771-862.

4. Kim H, Ahn JM, Kang DY, Lee J, Choi Y, Park SJ, Park DW. Management of Coronary Vulnerable Plaque With Medical Therapy or Local Preventive Percutaneous Coronary Intervention. *JACC Asia*. 2024;4:425-43.

5. Kraler S, Mueller C, Libby P, Bhatt DL. Acute coronary syndromes: mechanisms, challenges, and new opportunities. *Eur Heart J*. 2025;46:2866-89.

6. Escaned J, Lombardi M, Götberg M, Amabile N, Banning A, Barbato E, Brugaletta S, Chen SL, Doshi D, Koo BK, Kozuma K, Mahadevan K, Milasinovic D, Sinning JM, Toth G, Gonzalo N, Mamas MA, Kirtane AJ. Factors Contributing to Low Utilization of Intracoronary Imaging in Clinical Practice: A White Paper. *J Soc Cardiovasc Angiogr Interv*. 2025;4:103607.

7. Kim BK, Shin DH, Hong MK, Park HS, Rha SW, Mintz GS, Kim JS, Kim JS, Lee SJ, Kim HY, Hong BK, Kang WC, Choi JH, Jang Y; CTO-IVUS Study Investigators. Clinical Impact of Intravascular Ultrasound-Guided Chronic Total Occlusion Intervention With Zotarolimus-Eluting Versus Biolimus-Eluting Stent Implantation: Randomized Study. *Circ Cardiovasc Interv*. 2015;8:e002592.

8. Hong SJ, Kim BK, Shin DH, Nam CM, Kim JS, Ko YG, Choi D, Kang TS, Kang WC, Her AY, Kim YH, Hur SH, Hong BK, Kwon H, Jang Y, Hong MK; IVUS-XPL Investigators. Effect of Intravascular Ultrasound-Guided vs Angiography-Guided Everolimus-Eluting Stent Implantation: The IVUS-XPL Randomized Clinical Trial. *JAMA*. 2015;314:2155-63.

9. Zhang J, Gao X, Kan J, Ge Z, Han L, Lu S, Tian N, Lin S, Lu Q, Wu X, Li Q, Liu Z, Chen Y, Qian X, Wang J, Chai D, Chen C, Li X, Gogas BD, Pan T, Shan S, Ye F, Chen SL. Intravascular Ultrasound Versus Angiography-Guided Drug-Eluting Stent Implantation: The ULTIMATE Trial. *J Am Coll Cardiol*. 2018;72:3126-37.

10. Lee JM, Choi KH, Song YB, Lee JY, Lee SJ, Lee SY, Kim SM, Yun KH, Cho JY, Kim CJ, Ahn HS, Nam CW, Yoon HJ, Park YH, Lee WS, Jeong JO, Song PS, Doh JH, Jo SH, Yoon CH, Kang MG, Koh JS, Lee KY, Lim YH, Cho YH, Cho JM, Jang WJ, Chun KJ, Hong D, Park TK, Yang JH, Choi SH, Gwon HC, Hahn JY; RENOVATE-COMPLEX-PCI Investigators. Intravascular Imaging-Guided or Angiography-Guided Complex PCI. *N Engl J Med*. 2023;388:1668-79.

11. Holm NR, Andreasen LN, Neghabat O, Laanmets P, Kumsars I, Bennett J, Olsen NT, Odenstedt J, Hoffmann P, Dens J, Chowdhary S, O'Kane P, Bülow Rasmussen SH, Heigert M, Havndrup O, Van Kuijk JP, Biscaglia S, Mogensen LJH, Henareh L, Burzotta F, H Eek C, Mylotte D, Llinas MS, Koltowski L, Knaapen P, Calic S, Witt N, Santos-Pardo I, Watkins S, Lønborg J, Kristensen AT, Jensen LO, Calais F, Cockburn J, McNeice A, Kajander OA, Heestermans T, Kische S, Eftekhari A, Spratt JC, Christiansen EH; OCTOBER Trial Group. OCT or Angiography Guidance for PCI in Complex Bifurcation Lesions. *N Engl J Med*. 2023;389:1477-87.

12. Ali ZA, Landmesser U, Maehara A, Matsumura M, Shlofmitz RA, Guagliumi G, Price MJ, Hill JM, Akasaka T, Prati F, Bezerra HG, Wijns W, Leistner D, Canova P, Alfonso F, Fabbiocchi F, Dogan O, McGreevy RJ, McNutt RW, Nie H, Buccola J, West NEJ, Stone GW; ILUMIEN IV Investigators. Optical Coherence Tomography-Guided versus Angiography-Guided PCI. *N Engl J Med*. 2023;389:1466-76.

13. Li X, Ge Z, Kan J, Anjum M, Xie P, Chen X, Khan HS, Guo X, Saghir T, Chen J, Gill BUA, Guo N, Sheiban I, Raza A, Wei Y, Chen F, Mintz GS, Zhang JJ, Stone GW, Chen SL; IVUS-ACS Investigators. Intravascular ultrasound-guided versus angiography-guided percutaneous coronary intervention in acute coronary syndromes (IVUS-ACS): a two-stage, multicentre, randomised trial. *Lancet*. 2024;403:1855-65.

14. Hong SJ, Lee SJ, Lee SH, Lee JY, Cho DK, Kim JW, Kim SM, Hur SH, Heo JH, Jang JY, Koh JS, Won H, Lee JW, Hong SJ, Kim DK, Choe JC, Lee JB, Kim SJ, Yang TH, Lee JH, Hong YJ, Ahn JH, Lee YJ, Ahn CM, Kim JS, Ko YG, Choi D, Hong MK, Jang Y, Kim BK; OCCUPI investigators. Optical coherence tomography-guided versus angiography-guided percutaneous coronary intervention for patients with complex lesions (OCCUPI): an investigator-initiated, multicentre, randomised, open-label, superiority trial in South Korea. *Lancet*. 2024;404:1029-39.

15. Giacoppo D, Laudani C, Occhip$_{int}$i G, Spagnolo M, Greco A, Rochira C, Agnello F, Landolina D, Mauro MS, Finocchiaro S, Mazzone PM, Ammirabile N, Imbesi A, Raffo C, Buccheri S, Capodanno D. Coronary Angiography, Intravascular Ultrasound, and Optical Coherence Tomography for Guiding of Percutaneous Coronary Intervention: A Systematic Review and Network Meta-Analysis. *Circulation*. 2024;149:1065-86.

16. Byrne RA, Rossello X, Coughlan JJ, Barbato E, Berry C, Chieffo A, Claeys MJ, Dan GA, Dweck MR, Galbraith M, Gilard M, Hinterbuchner L, Jankowska EA, Jüni P, Kimura T, Kunadian V, Leosdottir M, Lorusso R, Pedretti RFE, Rigopoulos AG, Rubini Gimenez M, Thiele H, Vranckx P, Wassmann S, Wenger NK, Ibanez B; ESC Scientific Document Group. 2023 ESC Guidelines for the management of acute coronary syndromes. *Eur Heart J*. 2023;44:3720-826.

17. Neumann FJ, Sousa-Uva M, Ahlsson A, Alfonso F, Banning AP, Benedetto U, Byrne RA, Collet JP, Falk V, Head SJ, Jüni P, Kastrati A, Koller A, Kristensen SD, Niebauer J, Richter DJ, Seferović PM, Sibbing D, Stefanini GG, Windecker S, Yadav R, Zembala MO. 2018 ESC/EACTS Guidelines on myocardial revascularization. *EuroIntervention*. 2019;14:1435-534.

18. Pesarini G, Hellig F, Seth A, Shlofmitz RA, Ribichini FL. Percutaneous coronary intervention for calcified and resistant lesions. *EuroIntervention*. 2026;22:e339-55.

19. Wang X, Matsumura M, Mintz GS, Lee T, Zhang W, Cao Y, Fujino A, Lin Y, Usui E, Kanaji Y, Murai T, Yonetsu T, Kakuta T, Maehara A. In Vivo Calcium Detection by Comparing Optical Coherence Tomography, Intravascular Ultrasound, and Angiography. *JACC Cardiovasc Imaging*. 2017;10:869-79.

20. Amabile N, Rangé G, Landolff Q, Bressollette E, Meneveau N, Lattuca B, Levesque S, Boueri Z, Adjedj J, Casassus F, Belfekih A, Veugeois A, Souteyrand G, Honton B. OCT vs Angiography for Guidance of Percutaneous Coronary Intervention of Calcified Lesions: The CALIPSO Randomized Clinical Trial. *JAMA Cardiol*. 2025;10:666-75.

21. Fujino A, Mintz GS, Matsumura M, Lee T, Kim SY, Hoshino M, Usui E, Yonetsu T, Haag ES, Shlofmitz RA, Kakuta T, Maehara A. A new optical coherence tomography-based calcium scoring system to predict stent underexpansion. *EuroIntervention*. 2018;13:e2182-9.

22. Zhang M, Matsumura M, Usui E, Noguchi M, Fujimura T, Fall KN, Zhang Z, Nazif TM, Parikh SA, Rabbani LE, Kirtane AJ, Collins MB, Leon MB, Moses JW, Karmpaliotis D, Ali ZA, Mintz GS, Maehara A. Intravascular Ultrasound-Derived Calcium Score to Predict Stent Expansion in Severely Calcified Lesions. *Circ Cardiovasc Interv*. 2021;14:e010296.

23. Sato T, Matsumura M, Yamamoto K, Sugizaki Y, Shlofmitz E, Moses JW, Khalique OK, Thomas SV, Malik S, Dakroub A, Singh M, Shin D, Cohen DJ, Mintz GS, Shlofmitz RA, Jeremias A, Ali ZA, Maehara A. A Revised Optical Coherence Tomography-Derived Calcium Score to Predict Stent Underexpansion in Severely Calcified Lesions. *JACC Cardiovasc Interv*. 2025;18:622-33.

24. Virmani R, Kolodgie FD, Burke AP, Farb A, Schwartz SM. Lessons from sudden coronary death: a comprehensive morphological classification scheme for atherosclerotic lesions. *Arterioscler Thromb Vasc Biol*. 2000;20:1262-75.

25. Sato T, Matsumura M, Yamamoto K, Shlofmitz E, Moses JW, Khalique OK, Thomas SV, Tsoulios A, Cohen DJ, Mintz GS, Shlofmitz RA, Jeremias A, Ali ZA, Maehara A. Impact of Eruptive vs Noneruptive Calcified Nodule Morphology on Acute and Long-Term Outcomes After Stenting. *JACC Cardiovasc Interv*. 2023;16:1024-35.

26. Chau KW, Dakroub A, Shlofmitz ES, Shlofmitz RA, Jeremias A, Ali ZA. Recurrence of Protruding Calcified Nodule Visualized Using Optical Coherence Tomography Following Stent Implantation. *JACC Cardiovasc Interv*. 2023;16:1807-8.

27. Lim S, Cha JJ, Hong SJ, Kim JH, Joo HJ, Park JH, Yu CW, Ahn TH, Lim DS. Association between High Lipid Burden of Target Lesion and Slow TIMI Flow in Coronary Interventions. *J Clin Med*. 2022;11:5401.

28. Stone GW, Maehara A, Muller JE, Rizik DG, Shunk KA, Ben-Yehuda O, Genereux P, Dressler O, Parvataneni R, Madden S, Shah P, Brilakis ES, Kini AS; CANARY Investigators. Plaque Characterization to Inform the Prediction and Prevention of Periprocedural Myocardial Infarction During Percutaneous Coronary Intervention: The CANARY Trial (Coronary Assessment by Near-infrared of Atherosclerotic Rupture-prone Yellow). *JACC Cardiovasc Interv*. 2015;8:927-36.

29. Shlofmitz E, Iantorno M, Waksman R. Restenosis of Drug-Eluting Stents: A New Classification System Based on Disease Mechanism to Guide Treatment and State-of-the-Art Review. *Circ Cardiovasc Interv*. 2019;12:e007023.

30. Gonzalo N, Serruys PW, Okamura T, van Beusekom HM, Garcia-Garcia HM, van Soest G, van der Giessen W, Regar E. Optical coherence tomography patterns of stent restenosis. *Am Heart J*. 2009;158:284-93.

31. Ali ZA, Roleder T, Narula J, Mohanty BD, Baber U, Kovacic JC, Mintz GS, Otsuka F, Pan S, Virmani R, Sharma SK, Moreno P, Kini AS. Increased thin-cap neoatheroma and periprocedural myocardial infarction in drug-eluting stent restenosis: multimodality intravascular imaging of drug-eluting and bare-metal stents. *Circ Cardiovasc Interv*. 2013;6:507-17.

32. Stefanini GG, Alfonso F, Barbato E, Byrne RA, Capodanno D, Colleran R, Escaned J, Giacoppo D, Kunadian V, Lansky A, Mehilli J, Neumann FJ, Regazzoli D, Sanz-Sanchez J, Wijns W, Baumbach A. Management of myocardial revascularisation failure: an expert consensus document of the EAPCI. *EuroIntervention*. 2020;16:e875-90.

33. Han Y, Yuan X, Wang W, Wang N, Zhang Y, Jing J, Chen Y, Gao L. Clinical Significance of Optical Coherence Tomography-Guided Percutaneous Coronary Intervention for In-Stent Restenosis Within Drug-Eluting Stents: Impact on Patient Outcomes. *J Am Heart Assoc*. 2024;13:e033954.

34. Kubo T, Imanishi T, Takarada S, Kuroi A, Ueno S, Yamano T, Tanimoto T, Matsuo Y, Masho T, Kitabata H, Tsuda K, Tomobuchi Y, Akasaka T. Assessment of culprit lesion morphology in acute myocardial infarction: ability of optical coherence tomography compared with intravascular ultrasound and coronary angioscopy. *J Am Coll Cardiol*. 2007;50:933-9.

35. Pasupathy S, Air T, Dreyer RP, Tavella R, Beltrame JF. Systematic review of patients presenting with suspected myocardial infarction and nonobstructive coronary arteries. *Circulation*. 2015;131:861-70.

36. Heitner JF, Senthilkumar A, Harrison JK, Klem I, Sketch MH Jr, Ivanov A, Hamo C, Van Assche L, White J, Washam J, Patel MR, Bekkers SCAM, Smulders MW, Sacchi TJ, Kim RJ. Identifying the Infarct-Related Artery in Patients With Non-ST-Segment-Elevation Myocardial Infarction. *Circ Cardiovasc Interv*. 2019;12:e007305.

37. Reynolds HR, Maehara A, Kwong RY, Sedlak T, Saw J, Smilowitz NR, Mahmud E, Wei J, Marzo K, Matsumura M, Seno A, Hausvater A, Giesler C, Jhalani N, Toma C, Har B, Thomas D, Mehta LS, Trost J, Mehta PK, Ahmed B, Bainey KR, Xia Y, Shah B, Attubato M, Bangalore S, Razzouk L, Ali ZA, Merz NB, Park K, Hada E, Zhong H, Hochman JS. Coronary Optical Coherence Tomography and Cardiac Magnetic Resonance Imaging to Determine Underlying Causes of Myocardial Infarction With Nonobstructive Coronary Arteries in Women. *Circulation*. 2021;143:624-40.

38. Adlam D, Tweet MS, Gulati R, Kotecha D, Rao P, Moss AJ, Hayes SN. Spontaneous Coronary Artery Dissection: Pitfalls of Angiographic Diagnosis and an Approach to Ambiguous Cases. *JACC Cardiovasc Interv*. 2021;14:1743-56.

39. Jackson R, Al-Hussaini A, Joseph S, van Soest G, Wood A, Macaya F, Gonzalo N, Cade J, Caixeta A, Hlinomaz O, Leinveber P, O'Kane P, García-Guimaraes M, Cortese B, Samani NJ, Escaned J, Alfonso F, Johnson T, Adlam D. Spontaneous Coronary Artery Dissection: Pathophysiological Insights From Optical Coherence Tomography. *JACC Cardiovasc Imaging*. 2019;12:2475-88.

40. Xing L, Yamamoto E, Sugiyama T, Jia H, Ma L, Hu S, Wang C, Zhu Y, Li L, Xu M, Liu H, Bryniarski K, Hou J, Zhang S, Lee H, Yu B, Jang IK. EROSION Study (Effective Anti-Thrombotic Therapy Without Stenting: Intravascular Optical Coherence Tomography-Based Management in

Plaque Erosion): A 1-Year Follow-Up Report. *Circ Cardiovasc Interv.* 2017;10:e005860.

41. Jia H, Dai J, He L, Xu Y, Shi Y, Zhao L, Sun Z, Liu Y, Weng Z, Feng X, Zhang D, Chen T, Zhang X, Li L, Xu Y, Wu Y, Yang Y, Wang C, Li L, Li J, Hou J, Liu B, Mintz GS, Yu B. EROSION III: A Multicenter RCT of OCT-Guided Reperfusion in STEMI With Early Infarct Artery Patency. *JACC Cardiovasc Interv.* 2022;15:846-56.

42. Stone GW, Maehara A, Lansky AJ, de Bruyne B, Cristea E, Mintz GS, Mehran R, McPherson J, Farhat N, Marso SP, Parise H, Templin B, White R, Zhang Z, Serruys PW; PROSPECT Investigators. A prospective natural-history study of coronary atherosclerosis. *N Engl J Med.* 2011;364:226-35.

43. Calvert PA, Obaid DR, O'Sullivan M, Shapiro LM, McNab D, Densem CG, Schofield PM, Braganza D, Clarke SC, Ray KK, West NE, Bennett MR. Association between IVUS findings and adverse outcomes in patients with coronary artery disease: the VIVA (VH-IVUS in Vulnerable Atherosclerosis) Study. *JACC Cardiovasc Imaging.* 2011;4:894-901.

44. Cheng JM, Garcia-Garcia HM, de Boer SP, Kardys I, Heo JH, Akkerhuis KM, Oemrawsingh RM, van Domburg RT, Ligthart J, Witberg KT, Regar E, Serruys PW, van Geuns RJ, Boersma E. In vivo detection of high-risk coronary plaques by radiofrequency intravascular ultrasound and cardiovascular outcome: results of the ATHEROREMO-IVUS study. *Eur Heart J.* 2014;35:639-47.

45. Oemrawsingh RM, Cheng JM, García-García HM, van Geuns RJ, de Boer SP, Simsek C, Kardys I, Lenzen MJ, van Domburg RT, Regar E, Serruys PW, Akkerhuis KM, Boersma E; ATHEROREMO-NIRS Investigators. Near-infrared spectroscopy predicts cardiovascular outcome in patients with coronary artery disease. *J Am Coll Cardiol.* 2014;64:2510-8.

46. Waksman R, Di Mario C, Torguson R, Ali ZA, Singh V, Skinner WH, Artis AK, Cate TT, Powers E, Kim C, Regar E, Wong SC, Lewis S, Wykrzykowska J, Dube S, Kazziha S, van der Ent M, Shah P, Craig PE, Zou Q, Kolm P, Brewer HB, Garcia-Garcia HM; LRP Investigators. Identification of patients and plaques vulnerable to future coronary events with near-infrared spectroscopy intravascular ultrasound imaging: a prospective, cohort study. *Lancet.* 2019;394:1629-37.

47. Erlinge D, Maehara A, Ben-Yehuda O, Bøtker HE, Maeng M, Kjøller-Hansen L, Engstrøm T, Matsumura M, Crowley A, Dressler O, Mintz GS, Fröbert O, Persson J, Wiseth R, Larsen AI, Okkels Jensen L, Nordrehaug JE, Bleie Ø, Omerovic E, Held C, James SK, Ali ZA, Muller JE, Stone GW; PROSPECT II Investigators. Identification of vulnerable plaques and patients by intracoronary near-infrared spectroscopy and ultrasound (PROSPECT II): a prospective natural history study. *Lancet.* 2021;397:985-95.

48. Prati F, Romagnoli E, Gatto L, La Manna A, Burzotta F, Ozaki Y, Marco V, Boi A, Fineschi M, Fabbiocchi F, Taglieri N, Niccoli G, Trani C, Versaci F, Calligaris G, Ruscica G, Di Giorgio A, Vergallo R, Albertucci M, Biondi-Zoccai G, Tamburino C, Crea F, Alfonso F, Arbustini E. Relationship between coronary plaque morphology of the left anterior descending artery and 12 months clinical outcome: the CLIMA study. *Eur Heart J.* 2020;41:383-91.

49. Kedhi E, Berta B, Roleder T, Hermanides RS, Fabris E, IJsselmuiden AJJ, Kauer F, Alfonso F, von Birgelen C, Escaned J, Camaro C, Kennedy MW, Pereira B, Magro M, Nef H, Reith S, Al Nooryani A, Rivero F, Malinowski K, De Luca G, Garcia Garcia H, Granada JF, Wojakowski W. Thin-cap fibroatheroma predicts clinical events in diabetic patients with normal fractional flow reserve: the COMBINE OCT-FFR trial. *Eur Heart J.* 2021;42:4671-9.

50. Kubo T, Ino Y, Mintz GS, Shiono Y, Shimamura K, Takahata M, Terada K, Higashioka D, Emori H, Wada T, Kashiwagi M, Tanimoto T, Tanaka A, Hozumi T, Akasaka T. Optical coherence tomography detection of vulnerable plaques at high risk of developing acute coronary syndrome. *Eur Heart J Cardiovasc Imaging.* 2021;22:1376-84.

51. Jiang S, Fang C, Xu X, Xing L, Sun S, Peng C, Yin Y, Lei F, Wang Y, Li L, Chen Y, Pei X, Jia R, Tang C, Li S, Li S, Yu H, Chen T, Tan J, Liu X, Hou J, Dai J, Yu B. Identification of High-Risk Coronary Lesions by 3-Vessel Optical Coherence Tomography. *J Am Coll Cardiol.* 2023;81:1217-30.

52. Mol JQ, Volleberg RHJA, Belkacemi A, Hermanides RS, Meuwissen M, Protopopov AV, Laanmets P, Krestyaninov OV, Dennert R, Oemrawsingh RM, van Kuijk JP, Arkenbout K, van der Heijden DJ, Rasoul S, Lipsic E, Rodwell L, Camaro C, Damman P, Roleder T, Kedhi E, van Leeuwen MAH, van Geuns RM, van Royen N. Fractional Flow Reserve-Negative High-Risk Plaques and Clinical Outcomes After Myocardial Infarction. *JAMA Cardiol.* 2023;8:1013-21.

53. Nair A, Margolis MP, Kuban BD, Vince DG. Automated coronary plaque characterisation with intravascular ultrasound backscatter: ex vivo validation. *EuroIntervention.* 2007;3:113-20.

54. Madder RD, Steinberg DH, Anderson RD. Multimodality direct coronary imaging with combined near-infrared spectroscopy and intravascular ultrasound: initial US experience. *Catheter Cardiovasc Interv.* 2013;81:551-7.

55. Aguirre AD, Arbab-Zadeh A, Soeda T, Fuster V, Jang IK. Optical Coherence Tomography of Plaque Vulnerability and Rupture: JACC Focus Seminar Part 1/3. *J Am Coll Cardiol.* 2021;78:1257-65.

56. Vergallo R, Crea F. Atherosclerotic Plaque Healing. *N Engl J Med.* 2020;383:846-57.

57. Russo M, Fracassi F, Kurihara O, Kim HO, Thondapu V, Araki M, Shinohara H, Sugiyama T, Yamamoto E, Lee H, Vergallo R, Crea F, Biasucci LM, Yonetsu T, Minami Y, Soeda T, Fuster V, Jang IK. Healed Plaques in Patients With Stable Angina Pectoris. *Arterioscler Thromb Vasc Biol.* 2020;40:1587-97.

58. Del Val D, Berta B, Roleder T, Malinowski K, Bastante T, Hermanides RS, Wojakowski W, Fabris E, Cuesta J, De Luca G, Rivero F, Alfonso F, Kedhi E. Vulnerable plaque features and adverse events in patients with diabetes mellitus: a post hoc analysis of the COMBINE OCT-FFR trial. *EuroIntervention.* 2024;20:e707-17.

59. Chu M, Jia H, Gutiérrez-Chico JL, Maehara A, Ali ZA, Zeng X, He L, Zhao C, Matsumura M, Wu P, Zeng M, Kubo T, Xu B, Chen L, Yu B, Mintz GS, Wijns W, Holm NR, Tu S. Artificial intelligence and optical coherence tomography for the automatic characterisation of human atherosclerotic plaques. *EuroIntervention.* 2021;17:41-50.

60. Cheimariotis GA, Chatzizisis YS, Koutkias VG, Toutouzas K, Giannopoulos A, Riga M, Chouvarda I, Antoniadis AP, Doulaverakis C, Tsamboulatidis I, Kompatsiaris I, Giannoglou GD, Maglaveras N. ARCOCT: Automatic detection of lumen border in intravascular OCT images. *Comput Methods Programs Biomed.* 2017;151:21-32.

61. Matsumura M, Mintz GS, Dohi T, Li W, Shang A, Fall K, Sato T, Sugizaki Y, Chatzizisis YS, Moses JW, Kirtane AJ, Sakamoto H, Daida H, Minamino T, Maehara A. Accuracy of IVUS-Based Machine Learning Segmentation Assessment of Coronary Artery Dimensions and Balloon Sizing. *JACC Adv.* 2023;2:100564.

62. Ziemer PGP, Bulant CA, Orlando JI, Maso Talou GD, Álvarez LAM, Guedes Bezerra C, Lemos PA, García-García HM, Blanco PJ. Automated lumen segmentation using multi-frame convolutional neural networks in intravascular ultrasound datasets. *Eur Heart J Digit Health.* 2020;1:75-82.

63. Yu W, Tanigaki T, Ding D, Wu P, Du H, Ling L, Huang B, Li G, Yang W, Zhang S, Yan F, Okubo M, Xu B, Matsuo H, Wijns W, Tu S. Accuracy of Intravascular Ultrasound-Based Fractional Flow Reserve in Identifying Hemodynamic Significance of Coronary Stenosis. *Circ Cardiovasc Interv.* 2021;14:e009840.

64. Biccirè FG, Mannhart D, Kakizaki R, Windecker S, Räber L, Siontis GCM. Automatic assessment of atherosclerotic plaque features by intracoronary imaging: a scoping review. *Front Cardiovasc Med.* 2024;11:1332925.

65. Garg M, Garcia-Garcia HM, Calderón AT, Gupta J, Sortur S, Levine MB, Singla P, Picchi A, Sardella G, Adamo M, Frigoli E, Limbruno U, Rigattieri S, Diletti R, Boccuzzi G, Zimarino M, Contarini M, Russo F, Calabro P, Andò G, Varbella F, Garducci S, Palmieri C, Briguori C, Sánchez JS, Valgimigli M. Reproducibility of an artificial intelligence optical coherence tomography software for tissue characterization: Implications for the design of longitudinal studies. *Cardiovasc Revasc Med.* 2024;58:79-87.

66. Min HS, Yoo JH, Kang SJ, Lee JG, Cho H, Lee PH, Ahn JM, Park DW, Lee SW, Kim YH, Lee CW, Park SW, Park SJ. Detection of optical coherence tomography-defined thin-cap fibroatheroma in the coronary artery using deep learning. *EuroIntervention.* 2020;16:404-12.

67. Niioka H, Kume T, Kubo T, Soeda T, Watanabe M, Yamada R, Sakata Y, Miyamoto Y, Wang B, Nagahara H, Miyake J, Akasaka T, Saito Y, Uemura S. Automated diagnosis of optical coherence tomography imaging

on plaque vulnerability and its relation to clinical outcomes in coronary artery disease. *Sci Rep*. 2022;12:14067.

68. Chu M, De Maria GL, Dai R, Benenati S, Yu W, Zhong J, Kotronias R, Walsh J, Andreaggi S, Zuccarelli V, Chai J; Oxford Acute Myocardial Infarction (OxAMI) Study investigators; Channon K, Banning A, Tu S. DCCAT: Dual-Coordinate Cross-Attention Transformer for thrombus segmentation on coronary OCT. *Med Image Anal*. 2024;97:103265.

69. Park S, Araki M, Nakajima A, Lee H, Fuster V, Ye JC, Jang IK. Enhanced Diagnosis of Plaque Erosion by Deep Learning in Patients With Acute Coronary Syndromes. *JACC Cardiovasc Interv*. 2022;15:2020-31.

70. Tonino PA, De Bruyne B, Pijls NH, Siebert U, Ikeno F, van' t Veer M, Klauss V, Manoharan G, Engstrøm T, Oldroyd KG, Ver Lee PN, MacCarthy PA, Fearon WF; FAME Study Investigators. Fractional flow reserve versus angiography for guiding percutaneous coronary intervention. *N Engl J Med*. 2009;360:213-24.

71. De Bruyne B, Pijls NH, Kalesan B, Barbato E, Tonino PA, Piroth Z, Jagic N, Möbius-Winkler S, Rioufol G, Witt N, Kala P, MacCarthy P, Engström T, Oldroyd KG, Mavromatis K, Manoharan G, Verlee P, Frobert O, Curzen N, Johnson JB, Jüni P, Fearon WF; FAME 2 Trial Investigators. Fractional flow reserve-guided PCI versus medical therapy in stable coronary disease. *N Engl J Med*. 2012;367:991-1001.

72. Foley MJ, Rajkumar CA, Ahmed-Jushuf F, Simader F, Chotai S, Seligman H, Macierzanka K, Davies JR, Keeble TR, O'Kane P, Haworth P, Routledge H, Kotecha T, Clesham G, Williams R, Din J, Nijjer SS, Curzen N, Sinha M, Petraco R, Spratt J, Sen S, Cole GD, Harrell FE Jr, Howard JP, Francis DP, Shun-Shin MJ, Al-Lamee R; ORBITA-2 Investigators. Fractional Flow Reserve and Instantaneous Wave-Free Ratio as Predictors of the Placebo-Controlled Response to Percutaneous Coronary Intervention in Stable Coronary Artery Disease. *Circulation*. 2025;151:202-14.

73. Collet C, Collison D, Mizukami T, McCartney P, Sonck J, Ford T, Munhoz D, Berry C, De Bruyne B, Oldroyd K. Differential Improvement in Angina and Health-Related Quality of Life After PCI in Focal and Diffuse Coronary Artery Disease. *JACC Cardiovasc Interv*. 2022;15:2506-18.

74. Tanaka S, Noda T, Segawa T, Iwama M, Minagawa T, Watanabe S, Minatoguchi S. Relation between functional stenosis and tissue characterization of intermediate coronary plaques in patients with stable coronary heart disease. *J Cardiol*. 2010;55:296-302.

75. Sakai K, Mizukami T, Leipsic J, Belmonte M, Sonck J, Nørgaard BL, Otake H, Ko B, Koo BK, Maeng M, Jensen JM, Buytaert D, Munhoz D, Andreini D, Ohashi H, Shinke T, Taylor CA, Barbato E, Johnson NP, De Bruyne B, Collet C. Coronary Atherosclerosis Phenotypes in Focal and Diffuse Disease. *JACC Cardiovasc Imaging*. 2023;16:1452-64.

76. Tu S, Westra J, Adjedj J, Ding D, Liang F, Xu B, Holm NR, Reiber JHC, Wijns W. Fractional flow reserve in clinical practice: from wire-based invasive measurement to image-based computation. *Eur Heart J*. 2020;41:3271-9.

77. Yu W, Huang J, Jia D, Chen S, Raffel OC, Ding D, Tian F, Kan J, Zhang S, Yan F, Chen Y, Bezerra HG, Wijns W, Tu S. Diagnostic accuracy of intracoronary optical coherence tomography-derived fractional flow reserve for assessment of coronary stenosis severity. *EuroIntervention*. 2019;15:189-97.

78. Jeremias A, Maehara A, Matsumura M, Shlofmitz RA, Maksoud A, Akasaka T, Bezerra HG, Fearon WF, Samady H, Samuels B, Rapkin J, Gopinath A, Teraphongphom NT, Buccola J, Ali ZA. Optical Coherence Tomography-Based Functional Stenosis Assessment: FUSION-A Prospective Multicenter Trial. *Circ Cardiovasc Interv*. 2024;17:e013702.

79. Nakamura D, Wijns W, Price MJ, Jones MR, Barbato E, Akasaka T, Lee SW, Patel SM, Nishino S, Wang W, Gopinath A, Attizzani GF, Holmes D, Bezerra HG. New Volumetric Analysis Method for Stent Expansion and its Correlation With Final Fractional Flow Reserve and Clinical Outcome: An ILUMIEN I Substudy. *JACC Cardiovasc Interv*. 2018;11:1467-78.

80. Mauri L, Kereiakes DJ, Yeh RW, Driscoll-Shempp P, Cutlip DE, Steg PG, Normand SL, Braunwald E, Wiviott SD, Cohen DJ, Holmes DR Jr, Krucoff MW, Hermiller J, Dauerman HL, Simon DI, Kandzari DE, Garratt KN, Lee DP, Pow TK, Ver Lee P, Rinaldi MJ, Massaro JM; DAPT Study Investigators. Twelve or 30 months of dual antiplatelet therapy after drug-eluting stents. *N Engl J Med*. 2014;371:2155-66.

81. Ding D, Huang J, Westra J, Cohen DJ, Chen Y, Andersen BK, Holm NR, Xu B, Tu S, Wijns W. Immediate post-procedural functional assessment of percutaneous coronary intervention: current evidence and future directions. *Eur Heart J*. 2021;42:2695-707.

82. Andersen BK, Sejr-Hansen M, Maillard L, Campo G, Råmunddal T, Stähli BE, Guiducci V, Serafino LD, Escaned J, Santos IA, López-Palop R, Landmesser U, Dieu RS, Mejía-Rentería H, Koltowski L, Žiubrytė G, Cetran L, Adjedj J, Abdelwahed YS, Liu T, Mogensen LJH, Eftekhari A, Westra J, Lenk K, Casella G, Van Belle E, Biscaglia S, Olsen NT, Knaapen P, Kochman J, Santos RC, Scarsini R, Christiansen EH, Holm NR. Quantitative flow ratio versus fractional flow reserve for coronary revascularisation guidance (FAVOR III Europe): a multicentre, randomised, non-inferiority trial. *Lancet*. 2024;404:1835-46.

83. Park SJ, Ahn JM, Kang DY, Yun SC, Ahn YK, Kim WJ, Nam CW, Jeong JO, Chae IH, Shiomi H, Kao HL, Hahn JY, Her SH, Lee BK, Ahn TH, Chang KY, Chae JK, Smyth D, Mintz GS, Stone GW, Park DW; PREVENT Investigators. Preventive percutaneous coronary intervention versus optimal medical therapy alone for the treatment of vulnerable atherosclerotic coronary plaques (PREVENT): a multicentre, open-label, randomised controlled trial. *Lancet*. 2024;403:1753-65.

84. van Veelen A, Küçük IT, Garcia-Garcia HM, Fuentes FH, Kahsay Y, Delewi R, Beijk MAM, den Hartog AW, Grundeken MJ, Vis MM, Henriques JPS, Claessen BEPM. Paclitaxel-coated balloons for vulnerable lipid-rich plaques. *EuroIntervention*. 2024;20:e826-30.

85. Stone GW, Maehara A, Ali ZA, Held C, Matsumura M, Kjøller-Hansen L, Bøtker HE, Maeng M, Engstrøm T, Wiseth R, Persson J, Trovik T, Jensen U, James SK, Mintz GS, Dressler O, Crowley A, Ben-Yehuda O, Erlinge D; PROSPECT ABSORB Investigators. Percutaneous Coronary Intervention for Vulnerable Coronary Atherosclerotic Plaque. *J Am Coll Cardiol*. 2020;76:2289-301.

86. Mol JQ, Bom MJ, Damman P, Knaapen P, van Royen N. Pre-Emptive OCT-Guided Angioplasty of Vulnerable Intermediate Coronary Lesions: Results from the Prematurely Halted PECTUS-Trial. *J Interv Cardiol*. 2020;2020:8821525.

87. Burzotta F, Leone AM, Aurigemma C, Zambrano A, Zimbardo G, Arioti M, Vergallo R, De Maria GL, Cerracchio E, Romagnoli E, Trani C, Crea F. Fractional Flow Reserve or Optical Coherence Tomography to Guide Management of Angiographically Intermediate Coronary Stenosis: A Single-Center Trial. *JACC Cardiovasc Interv*. 2020;13:49-58.

88. Yu M, Yang Y, Dong SL, Zhao C, Yang F, Yuan YF, Liao YH, He SL, Liu K, Wei F, Jia HB, Yu B, Cheng X. Effect of Colchicine on Coronary Plaque Stability in Acute Coronary Syndrome as Assessed by Optical Coherence Tomography: The COLOCT Randomized Clinical Trial. *Circulation*. 2024;150:981-93.

89. Psaltis PJ, Nguyen MT, Singh K, Sinhal A, Wong DTL, Alcock R, Rajendran S, Dautov R, Barlis P, Patel S, Salagaras T, Marathe JA, Bursill CA, Montarello NJ, Nidorf SM, Thompson PL, Butters J, Cuthbert AR, Yelland LN, Ottaway JL, Kataoka Y, Di Giovanni G, Nicholls SJ. Optical coherence tomography assessment of the impact of colchicine on non-culprit coronary plaque composition after myocardial infarction. *Cardiovasc Res*. 2025;121:468-78.

90. Kini AS. Effect of Evolocumab on Coronary Plaque Characteristics in Stable Coronary Artery Disease: A Multimodality Imaging Study (The YELLOW III Study). ACC 2023. 4-6 March 2023. New Orleans, LA, USA.

91. Koo BK, Hu X, Kang J, Zhang J, Jiang J, Hahn JY, Nam CW, Doh JH, Lee BK, Kim W, Huang J, Jiang F, Zhou H, Chen P, Tang L, Jiang W, Chen X, He W, Ahn SG, Yoon MH, Kim U, Lee JM, Hwang D, Ki YJ, Shin ES, Kim HS, Tahk SJ, Wang J; FLAVOUR Investigators. Fractional Flow Reserve or Intravascular Ultrasonography to Guide PCI. *N Engl J Med*. 2022;387:779-89.

92. Ding D, Zhang J, Wu P, Wang Z, Shi H, Yu W, Hu X, Kang J, Hahn JY, Nam CW, Doh JH, Lee BK, Kim W, Huang J, Jiang F, Zhou H, Chen P, Tang L, Jiang W, Chen X, He W, Ahn SG, Yoon MH, Kim U, Ki YJ, Shin ES, Tahk SJ, Pu J, Wijns W, Wang J, Koo BK, Tu S. Prognostic Value of Postpercutaneous Coronary Intervention Murray-Law-Based Quantitative Flow Ratio: Post Hoc Analysis From FLAVOUR Trial. *JACC Asia*. 2025;5:59-70.

93. Verheye S, Roth L, De Meyer I, Van Hove CE, Nahon D, Santoianni D, Yianni J, Martinet W, Buchbinder M, De Meyer GR. Cryotherapy increases

features of plaque stability in atherosclerotic rabbits. *EuroIntervention*. 2016;12:748-56.

94. Wang KL, Balmforth C, Meah MN, Daghem M, Moss AJ, Tzolos E, Kwiecinski J, Molek-Dziadosz P, Craig N, Bularga A, Adamson PD, Dawson DK, Arumugam P, Sabharwal NK, Greenwood JP, Townend JN, Calvert PA, Rudd JHF, Verjans JW, Berman DS, Slomka PJ, Dey D, Mills NL, van Beek EJR, Williams MC, Dweck MR, Newby DE; PRE(18) FFIR Study Investigators. Coronary Atherosclerotic Plaque Activity and Risk of Myocardial Infarction. *J Am Coll Cardiol*. 2024;83:2135-44.

95. Chhatriwalla AK, Nicholls SJ, Nissen SE. The ASTEROID trial: coronary plaque regression with high-dose statin therapy. *Future Cardiol*. 2006;2:651-4.

96. Räber L, Ueki Y, Otsuka T, Losdat S, Häner JD, Lonborg J, Fahrni G, Iglesias JF, van Geuns RJ, Ondracek AS, Radu Juul Jensen MD, Zanchin C, Stortecky S, Spirk D, Siontis GCM, Saleh L, Matter CM, Daemen J, Mach F, Heg D, Windecker S, Engstrøm T, Lang IM, Koskinas KC; PACMAN-AMI collaborators. Effect of Alirocumab Added to High-Intensity Statin Therapy on Coronary Atherosclerosis in Patients With Acute Myocardial Infarction: The PACMAN-AMI Randomized Clinical Trial. *JAMA*. 2022;327:1771-81.

97. Biccirè FG, Häner J, Losdat S, Ueki Y, Shibutani H, Otsuka T, Kakizaki R, Hofbauer TM, van Geuns RJ, Stortecky S, Siontis GCM, Bär S, Lønborg J, Heg D, Kaiser C, Spirk D, Daemen J, Iglesias JF, Windecker S, Engstrøm T, Lang I, Koskinas KC, Räber L. Concomitant Coronary Atheroma Regression and Stabilization in Response to Lipid-Lowering Therapy. *J Am Coll Cardiol*. 2023;82:1737-47.

98. Laudani C, Occhip$_{int}$i G, Greco A, Giacoppo D, Spagnolo M, Capodanno D. A pairwise and network meta-analysis of anti-inflammatory strategies after myocardial infarction: the TITIAN study. *Eur Heart J Cardiovasc Pharmacother*. 2025;11:218-29.

99. Isidori F, Lella E, Marco V, Albertucci M, Ozaki Y, La Manna A, Biccirè FG, Romagnoli E, Bourantas CV, Paoletti G, Fabbiocchi F, Gatto L, Budassi S, Sticchi A, Burzotta F, Taglieri N, Calligaris G, Arbustini E, Alfonso F, Prati F. Adoption of a new automated optical coherence tomography software to obtain a lipid plaque spread-out plot. *Int J Cardiovasc Imaging*. 2021;37:3129-35.

100. Biccirè FG, Budassi S, Ozaki Y, Boi A, Romagnoli E, Di Pietro R, Bourantas CV, Marco V, Paoletti G, Debelak C, Sammartini E, Versaci F, Fabbiocchi F, Burzotta F, Pastori D, Crea F, Arbustini E, Alfonso F, Prati F. Optical coherence tomography-derived lipid core burden index and clinical outcomes: results from the CLIMA registry. *Eur Heart J Cardiovasc Imaging*. 2023;24:437-45.

101. Hong H, Jia H, Zeng M, Gutiérrez-Chico JL, Wang Y, Zeng X, Qin Y, Zhao C, Chu M, Huang J, Liu L, Hu S, He L, Chen L, Wijns W, Yu B, Tu S. Risk Stratification in Acute Coronary Syndrome by Comprehensive Morphofunctional Assessment With Optical Coherence Tomography. *JACC Asia*. 2022;2:460-72.

102. Yang F, Li C, Tan Q, Yu W, De Maria GL, Wang F, Wu J, Tu S. In Vivo Quantitative Imaging of Coronary Blood Flow by Intracoronary Doppler OCT. *IEEE Trans Biomed Eng*. 2025;72:1665-73.

103. Stone PH, Saito S, Takahashi S, Makita Y, Nakamura S, Kawasaki T, Takahashi A, Katsuki T, Nakamura S, Namiki A, Hirohata A, Matsumura T, Yamazaki S, Yokoi H, Tanaka S, Otsuji S, Yoshimachi F, Honye J, Harwood D, Reitman M, Coskun AU, Papafaklis MI, Feldman CL; PREDICTION Investigators. Prediction of progression of coronary artery disease and clinical outcomes using vascular profiling of endothelial shear stress and arterial plaque characteristics: the PREDICTION Study. *Circulation*. 2012;126:172-81.

104. Morgan B, Murali AR, Preston G, Sima YA, Marcelo Chamorro LA, Bourantas C, Torii R, Mathur A, Baumbach A, Jacob MC, Karabasov S, Krams R. A physics-based machine learning technique rapidly reconstructs the wall-shear stress and pressure fields in coronary arteries. *Front Cardiovasc Med*. 2023;10:1221541.

105. Gu SZ, Ahmed ME, Huang Y, Hakim D, Maynard C, Cefalo NV, Coskun AU, Costopoulos C, Maehara A, Stone GW, Stone PH, Bennett MR. Comprehensive biomechanical and anatomical atherosclerotic plaque metrics predict major adverse cardiovascular events: A new tool for clinical decision making. *Atherosclerosis*. 2024;390:117449.

106. Ali ZA, Dager A, Zúñiga M, Fonseca J, Arana C, Chamié D, Hill JM, Madder RD, Muller JE, Simonton CA, Tearney GJ, Stone GW. First-in-Human Experience With a Novel Multimodality DeepOCT-NIRS Intracoronary Imaging System. *J Soc Cardiovasc Angiogr Interv*. 2024;3:101344.

107. Tufaro V, Jaffer FA, Serruys PW, Onuma Y, van der Steen AFW, Stone GW, Muller JE, Marcu L, Van Soest G, Courtney BK, Tearney GJ, Bourantas CV. Emerging Hybrid Intracoronary Imaging Technologies and Their Applications in Clinical Practice and Research. *JACC Cardiovasc Interv*. 2024;17:1963-79.

108. Kim JH, Song JW, Kim YH, Kim HJ, Kim RH, Park YH, Nam HS, Kang DO, Yoo H, Park K, Kim JW. Multimodal Imaging-Assisted Intravascular Theranostic Photoactivation on Atherosclerotic Plaque. *Circ Res*. 2024;135:e114-32.

109. He L, Qin Y, Xu Y, Hu S, Wang Y, Zeng M, Feng X, Liu Q, Syed I, Demuyakor A, Zhao C, Chen X, Li Z, Meng W, Xu M, Liu H, Ma L, Dai J, Xing L, Yu H, Hou J, Jia H, Mintz GS, Yu B. Predictors of non-stenting strategy for acute coronary syndrome caused by plaque erosion: four-year outcomes of the EROSION study. *EuroIntervention*. 2021;17:497-505.

110. Motreff P, Malcles G, Combaret N, Barber-Chamoux N, Bouajila S, Pereira B, Amonchot A, Citron B, Lusson JR, Eschalier R, Souteyrand G. How and when to suspect spontaneous coronary artery dissection: novel insights from a single-centre series on prevalence and angiographic appearance. *EuroIntervention*. 2017;12:e2236-43.

Supplementary data

Supplementary Table 1. Intracoronary imaging calcium scoring systems.

Supplementary Table 2. Intracoronary imaging classification of stent failure.

Supplementary Table 3. Longitudinal natural history cohort studies to identify plaque characteristics, as assessed with intracoronary imaging, associated with adverse clinical outcomes.

The supplementary data are published online at: https://eurointervention.pcronline.com/doi/10.4244/EIJ-D-25-00266

Supplementary data

Supplementary Table 1. Intracoronary imaging calcium scoring systems.

Classification	Modality	Calcium Arc	Calcium thickness	Calcium Length	Calcified Nodule	Total Score
Fujino A et al.	OCT	>180°: 2 points	>0.5 mm: 1 point	>5 mm: 1 point	-	**4**
Zhang M et al.	IVUS	>270°: 1 point	-	Present: 1 point	Present: 1 point	**2**
Sato et al.	OCT	360°: 1 point	>0.3mm: 1point	Arc >270° for >3mm: 1 point	-	**3**
IVUS: Intravascular ultrasound; OCT Optical coherence tomography						

Supplementary Table 2. Intracoronary imaging classification of stent failure.

Classification								
Waksman **(IVUS±OCT)**	**Type 1A**	**Type 1B**	**Type 2A**	**Type 2B**	**Type 2 C**	**Type 3**	**Type 4**	**Type 5**
	Underexpansion	Stent fracture	Intimal hyperplasia	Neoatherosclerosis non-calcified	Neoatherosclerosis calcified	Mixed pattern	CTO	2 stent layers
Gonzalo N et al. **(OCT)**	**Restenotic Tissue Structure**	**Restenotic Tissue Backscatter**	**Microvessels**		**Lumen shape**		**Presence of intra-luminal material**	
	1. Homogeneous 2. Heterogeneous 3. Layered	1. High 2. Low	1. Present 2. Absent		1. Regular 2. Irregular		1. Present 2. Absent	
Ali ZA et al. **(OCT)**	**Type1**	**Type 2**	**Type 3**		**Type 4**			
	Thin cap neoatheroma	Thick cap neoatheroma	Per-strut neoatheroma		Pre-existing fibroatheroma			
CTO: Chronic total occlusion; IVUS: Intravascular ultrasound; OCT Optical coherence tomography								

Supplementary Table 3. Longitudinal natural history cohort studies to identify plaque characteristics, as assessed with intracoronary imaging, associated with adverse clinical outcomes.

Study	Cohort, (n)	IC Imaging Modality	Follow-up, months	Key Endpoint	Endpoint Events	Key Predictors of Primary Endpoint
PROSPECT (2011)	Non-culprit lesions; ACS admission 697 patients	RF-IVUS *20MHz Eagle Eye, Phillips Volcano*	40mnths	**MACE** (Composite of non-culprit cardiac death, cardiac arrest, MI or hospitalisation due to unstable or progressive angina)	149 events in 134 patients	Plaque burden ≥70%: **HR 5.03** (95%CI 2.51-10.11) RF-IVUS defined TCFA: **HR 3.35** (95%CI 1.77-6.36) MLA ≤4.0mm^2: **HR 3.21** (95%CI 1.61-6.42)
VIVA (2011)	Non-culprit lesions; ACS & CCS 167 patients	RF-IVUS *20MHz Eagle Eye, Phillips Volcano*	20mnths (median)	**MACE** (Composite of all-cause death, non-culprit MI or unplanned revascularisation excluding ISR)	13 events in 167 patients	RF-IVUS defined TCFA: **HR 1.79** (95%CI 1.20-2.66)
ATHEROREMO-IVUS (2014)	Non-culprit lesions; ACS & CCS 581 patients	RF-IVUS *20MHz Eagle Eye, Phillips Volcano*	12mnths	**MACE** (Composite of non-culprit related or inderterminate mortality, ACS or unplanned revascularisation)	45 events in 581 patients	Plaque burden ≥70%: **HR 2.90** (95%CI 1.15-5.49) RF-IVUS defined TCFA: **HR 1.98** (95%CI 1.09-3.60) *MLA ≤4.0mm^2: **HR 1.23** (95%CI 0.67-2.26)*
ATHEROREMO-NIRS (2014)	Non-culprit lesions; ACS & CCS 203 patients	NIRS only *InfraredX, Nipro*	12mnths	**MACE** (Composite of all cause death, non-culprit non-fatal ACS, stroke, or unplanned non-culprit revascularisation)	21 events in 203 patients	LCBI$_{vessel}$ >43 HR 4.04 (95%CI 1.33-12.29)
LRP (2019)	Non-culprit lesions; ACS & CCS 1271 patients	NIRS-IVUS *40MHz InfraredX, Nipro*	24mnths	**MACE** (Composite of non-culprit cardiac death, cardiac arrest, non-fatal MI or ACS, unplanned revascularisation or >20% diameter stenosis progression and unrelated to treatment at index procedure)	103 events in 1271 patients	Plaque burden ≥70% (within maxLCBI$_{4mm}$): **HR 3.99** (95%CI 1.38-11.56) MLA ≤4.0mm^2 (within maxLCBI$_{4mm}$: **HR 1.79** (95%CI 1.02-3.16) Max LCBI4$_{mm}$ >400: **HR 3.35** (95%CI 1.77-6.36)
PROSPECT II (2021)	Non-culprit lesion; MI within 4 weeks 902 patients	NIRS-IVUS *40MHz InfraredX, Nipro*	48mnths	**MACE** (Composite of non-culprit related cardiac death, myocardial infarction, unstable angina, or progressive angina requiring revascularisation or with rapid lesion progression)	66 events in 898 patients	Plaque burden ≥70%: **HR 3.49** (95%CI 1.83-6.63) MLA ≤4.0mm^2: **HR 6.00** (95%CI 2.12-17.00) Max LCBI4$_{mm}$ ≥324.7: **HR 2.27** (95%CI 1.25-4.13)

CLIMA (2019)	Non-culprit LAD lesions; ACS & CCS 1003 patients	OCT *St Jude / Abbott Vascular*	12mnths	**Cardiac death & LAD lesion related MI**	37 events in 1003 patients	'High-risk' plaque: **HR 7.54** (95%CI 3.1-18.6) *High risk plaque defined as (all of):* *i. Lipid arc >180°* *ii. Minimal fibrous cap thickness <75µm* *iii. Minimum lumen area <3.50mm²* *iv. Macrophage infiltration*
COMBINE-OCT (2021)	FFR ≥0.80 non-culprit lesions in patients with T2DM; ACS & CCS 390 patients	OCT *St Jude / Abbott Vascular*	18mnths	**Non-culprit lesion MACE** (Composite of cardiac death, non-culprit lesion MI, clinically driven non-culprit lesion revascularisation or hospitalisation due to unstable or progressive angina)	22 events in 390 patients	Thin-capped fibroatheroma: **HR 2.63** (95%CI 1.64-4.23) *Thin-capped fibroatheroma defined as:* *i. Fibrous cap thickness ≤65µm* *ii. Lipid arc >90°*
Kubo et al (2021)	Non-culprit lesions; ACS & CCS 1378 patients	OCT *Terumo / Abbott Vascular*	55mnths (median)	**Non-culprit related ACS**	129 events in 1378 patients	'High-risk' plaque: **HR 2.63** (95%CI 1.64-4.23) *High risk plaque defined as (all of):* *i. Lipid arc ≥185°* *ii. Minimal fibrous cap thickness <150µm* *iii. Minimum lumen area ≤2.90mm²*
Jiang et al (2023)	Non-culprit lesions; ACS admission 883 patients	OCT *Abbott Vascular*	40mnths (median)	**MACE** (Composite of cardiac death, non-culprit related non-fatal MI, or unplanned coronary revascularisation)	50 events in 883 patients	Thin-capped fibroatheroma: **HR 3.15** (95%CI 1.77-5.61) Minimum lumen area <3.50mm²: **HR 3.57 (**95%CI 1.42-8.99) TCFA & MLA <3.5mm²: **HR 5.23** (95%CI 2.98-9.17) *Thin-capped fibroatheroma defined as:* *i. Fibrous cap thickness ≤65µm* *ii. Lipid arc >90°*
PECTUS-obs (2023)	FFR ≥0.80 non-culprit lesions; ACS admission 420 patients	OCT *Device manufacturer not stated*	24mnths	**MACE** (Composite of all-cause mortality, non-fatal MI, or unplanned revascularisation)	45 events in 420 patients	'High-risk' plaque: **HR 1.99** (95%CI 1.10-3.61) *High risk plaque defined as (2 of):* *i. Lipid arc ≥90°* *ii. Minimal fibrous cap thickness <65µm* iii. *Plaque rupture or thrombus present*

ACS: Acute coronary syndrome; CCS: Chronic coronary syndrome; FFR: Fractional flow reserve; ISR: In-stent restenosis; LAD: Left anterior descending artery; LCBI: Lipid core burden index; MACE: Major adverse cardiovascular events; MHz: Megahertz; MI: Myocardial infarction; MLA: Minimum lumen area; NIRS: Near infrared spectroscopy; OCT: Optical coherence tomography; PCI: Percutaneous coronary intervention; RF-IVUS: Radiofrequency intravascular ultrasound; TCFA: Thin-capped fibroatheroma; T2DM:Type II diabetes mellitus